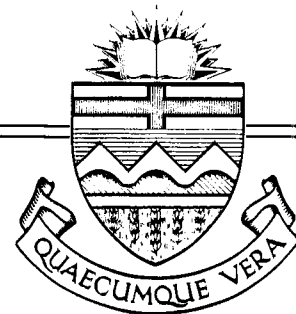# BEHAVIOUR OF WELDED CONNECTIONS UNDER COMBINED SHEAR AND MOMENT

by
J. L. DAWE
and
G. L. KULAK

June, 1972

RECENT STRUCTURAL ENGINEERING REPORTS

Department of Civil Engineering

University of Alberta.

24. *Prestressed Concrete Beams with Web Reinforcement under Combined Loading* by P. Mukherjee and J. Warwaruk, May 1970.

25. *Studies of Reinforced Concrete Shear Wall-Frame Structures* by R.P. Nikhed, J.G. MacGregor and P.F. Adams, June 1970.

26. *Buckling Strengths of Hot Rolled Hat Shaped Sections* by D.A. Heaton and P.F. Adams, July 1970.

27. *Experimental and Analytical Investigation of the Behavior of Coupled Shear Wall-Frame Structures* by S.N.G. Majumdar and P.F. Adams, August 1970.

28. *Comparative Study of Slab-Beam Systems* by J. Misic and S.H. Simmonds, September, 1970.

29. *Elastic-Plastic Analysis of Three Dimensional Structures* by J.H. Wynhoven and P.F. Adams, September 1970.

30. *Flexural and Lateral-Torsional Buckling Strengths and Double Angle Struts* by N.J. Nuttall and P.F. Adams, September 1970.

31. *Stiffness Influence Coefficients for Non-Axisymmetrical Loading on Closed Cylindrical Shells* by S.H. Iyer and S.H. Simmonds, October 1970.

32. *CSA-S16-1969 Steel Structures for Buildings - Seminar Notes* by P.F. Adams, G.L. Kulak and J. Longworth, November 1970.

33. *Experiments on Steel Wide-Flange Beam-Columns Subjected to Lateral Loads* by G.W. English and P.F. Adams, May 1971.

34. *Finite Element Analysis of Thin-Walled Members of Open Section* by S. Rajasekaran, September 1971.

35. *Finite Element Programs for Beam Analysis* by S. Rajasekaran, September 1971.

36. *Seminar on Building Code Requirements, ACI-318-71* by J.G. MacGregor, S.H. Simmonds and J. Warwaruk, July 1971.

37. *Stability of Braced Frames* by J.H. Davison and P.F. Adams, October 1971.

38. *Time Dependent Deflections of Reinforced Concrete Slabs* by A. Scanlon and D.W. Murray, December 1971.

39. *Fatigue of Reinforcing Bars* by I.C. Jhamb and J.G. MacGregor, February 1972.

40. *Behavior of Welded Connections Under Combined Shear and Moment* by J.L. Dawe and G.L. Kulak, June 1972.

BEHAVIOUR OF WELDED CONNECTIONS UNDER COMBINED

SHEAR AND MOMENT

by

J.L. Dawe

G.L. Kulak

DEPARTMENT OF CIVIL ENGINEERING

THE UNIVERSITY OF ALBERTA

EDMONTON, ALBERTA

JUNE, 1972

A B S T R A C T

Current working stress design methods as applied
to eccentrically loaded welded connections have been shown
to result in high factors of safety. The currently accepted
method for the design of eccentrically loaded welded connections
has been in vogue for almost thirty years now, and no con-
sideration has been given to the fact that transverse fillet
welds are approximately 30 per cent stronger than longitudinal
fillet welds. Recently, a rational theoretical method of
predicting the ultimate capacity of fillet welded connections
under combined shear and torsion was presented.

In the present work, this method has been extended
to the case in which rotational deformation is prevented in
the compression zone of the weld. Initially, the validity
of this method was established by comparing predicted
ultimate loads with actual test loads obtained for a series
of eight eccentrically loaded connections consisting of two
vertical lines of fillet weld. The results show that the
predicted loads for these specimens compare favourably with
the actual test loads. The theoretical method and the testing
program were then extended to include a T-shaped weld

connection and an I-shaped weld connection. Favourable correlation between predicted loads and test loads for these specimens was also obtained. In addition, the theoretical method was extended to predict the capacities for a number of hypothetical cases.

The study shows that the factor of safety, as provided for by present design methods for the eccentrically loaded fillet welded connections used in the test program, is high and somewhat inconsistent. This illustrates the fact that the present design methods used in this area are inadequate and not strictly applicable to fillet welds whose strength depends on the angle of loading of the individual elements comprising the overall weld. By making use of the more accurate ultimate load analysis based on the true load versus deformation response of elemental fillet welds it is possible to reduce these high safety factors and bring them more in line with those of other structural elements.

A C K N O W L E D G E M E N T S

TABLE OF CONTENTS

1. INTRODUCTION

1.1 General

A connection loaded eccentrically results when the line of action of the resultant load to be resisted by a joint does not pass through the centroid of the resisting elements. In all such cases the fasteners are subjected to secondary stresses induced by the moment effect of the eccentric load. Eccentric loading of connections is often unavoidable and in such cases it is necessary to account for the moment-induced stresses. Eccentric connections occur in beam-to-column connections, web splice connections of beams, and bracket supports attached to column flanges. Typical examples of such connections are shown in Fig. 1.1.

In many eccentrically loaded welded connections, the weld is free to deform above and below the neutral axis of the weld group. In other practical instances it may be necessary to form eccentric connections in which the weld is not free to rotate in the compression zone because of direct bearing between the connected plates.

Fig. 1.1(a) shows a connection in which the fillet weld is free to deform throughout its length. In this case, the neutral axis would be at mid-depth of a symmetrical weld arrangement. In the connections illustrated in Fig. 1.1(b) and (c), the weld in the compression zone cannot deform

under rotational movement and the connected plates are in bearing beyond the point of an initial set in the weld.

The current design procedures[1,7,8,17,19] used for eccentrically loaded welded connections are based on the procedures formerly used to analyse riveted joints.[3] The welds are designed to transmit a direct shear stress and a moment-induced shear stress based on ordinary elastic beam analysis. These two stresses are combined vectorially and then compared with the allowable stress on the throat area of the weld. This approach assumes that the response of the weld to the load is elastic.

Even with the recent increase[1,9] in allowable shear stress on the effective throat area of the weld, this procedure will result in a high factor of safety based on the ultimate strength of the weld.[3,18] It would be desirable therefore to develop a suitable method for analysing the ultimate strength of eccentrically loaded welded connections, and thereby reduce this high factor of safety. Knowledge of the ultimate strength of a welded connection would also enable designers to make a more rational choice between a welded connection and a bolted connection since the ultimate strength of a bolted connection under eccentric loading can be accurately obtained.[12,13,15,17]

In 1969, Butler and Kulak[5] presented a method for predicting the ultimate capacity of eccentrically loaded welded connections in which the weld is free to deform throughout its length. The method was based upon the actual load - deformation response of elemental lengths of fillet weld for which an empirical relationship was established. In the present investigation, the principles of this method were used to analyse welded connections in which the weld could not rotate in the compression zone.

1.2 Objectives

The objectives of this investigation are:

1. to develop a method for accurately determining the ultimate strength of eccentrically loaded welded connections in which the weld in the compression zone is not free to rotate.

2. to verify the analytical method by the results of a suitable testing program.

3. to evaluate the present design procedures governing the design of this type of connection.

1.3 Scope

The analytical study deals with eccentrically loaded fillet welded connections in which the weld in the

compression zone is not free to deform under moment-induced stresses. The investigation includes a critical review of current allowable stress design procedures for this type of connection. The proposed analytical procedure recognises the true load - deformation response of elemental lengths of fillet weld as formulated empirically by Butler and Kulak.[6]

Tests have shown that a fillet weld loaded perpendicular to its axis is approximately 30 per cent stronger than if it were loaded parallel to its axis and that the strength is intermediate for angles in between.[6,20] Present design provisions do not consider this added strength (and reduced ductility).[7,17,19] In the method outlined herein, this property of fillet welds is considered and the mathematical analysis incorporates the effect of different angles of load with respect to the weld element.

Three series of tests on full-size specimens were conducted. The weld configuration was varied for the three series of tests but the basic characteristic of rotational non-deformability of weld in the compression zone was maintained throughout. The variables were the length of weld, the eccentricity of load, and the area provided for bearing in the compression zone. A full description of these specimens is given in Chapter IV. Such variables as residual

stresses and stress concentrations were not considered. It is felt that these variables in the experimental spec- imens will exist to about the same degree in actual structural connections.

In order to establish confidence in the analytic procedure developed herein, Test Series One was established. The eight full-size specimens of this series consisted of simple vertical fillet welds connecting a plate to a column flange. The predicted loads and the actual test loads compare favourably and therefore the program has been extended to include a T-shaped weld configuration (Series Two) and an I-shaped weld configuration (Series Three). The results of these tests also compare favourably with the predicted loads. The results of all these tests are dis- cussed in Chapter V.

The empirical relationships used in the analytical procedure were adjusted to conform to the particular char- acteristics of strength and deformability of the welds used. The adjustment factors were obtained by testing control coupons made from the same type of weld as used in each series of full-size specimens. The welds were tested at a loading angle of zero degrees to the weld axis and the results were used to modify the empirical relationships presented by Butler and Kulak[6] for other values of the load angle.

A computer program presented in Appendix B may be used to calculate the ultimate capacity of an eccentrically loaded welded connection in which the weld is not free to rotate in the compression zone. This program may be used for the simple line-shaped weld configuration only. It may be easily modified so as to obtain ultimate capacities for T-shaped or I-shaped weld configurations. For example, the mathematical procedure for analysing T-shaped weld configurations has been outlined in Appendix D. The empirical relationships used in the computer program are based on the test results presented herein.
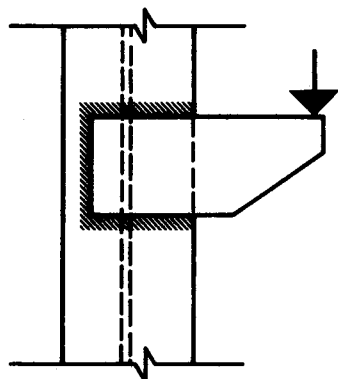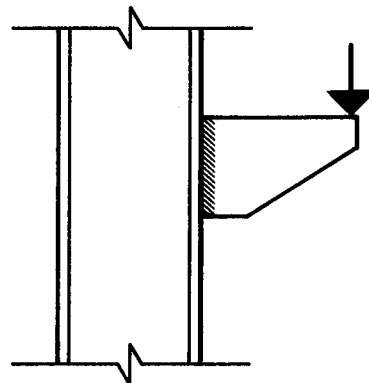
a. BRACKET CONNECTION   b. BRACKET CONNECTION
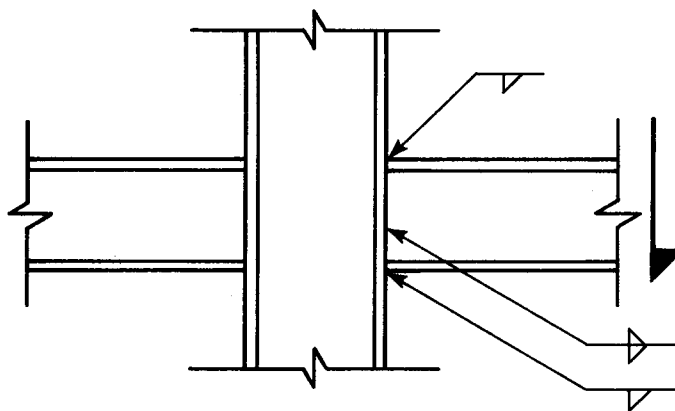
c. BEAM-TO-COLUMN CONNECTION

FIG. I.I TYPICAL ECCENTRICALLY LOADED CONNECTIONS

2. L I T E R A T U R E   S U R V E Y

2.1 Current Methods of Analysis

Present design methods commonly used for fillet-welded connections under eccentric loading assume that the load - deformation response for the weld is linear and that a proportional limit is not exceeded. The concept of an elastic beam element is used to obtain bending and shear stresses existing in the weld. The remainder of this chapter summarises these procedures and uses an example for the purpose of illustration.

As has been mentioned, some connections are such that the weld is not free to deform in the compression zone. Current methods for the design of such connections consider a line of weld to be an elastic beam element subjected to flexural stresses defined by the relationship,

$$\sigma = \frac{My}{I} \qquad (2.1)$$

vectorially combined with a direct shear stress given by,

$$\tau = \frac{P}{A} \qquad (2.2)$$

where,

     M = the product of the load, P, and its

        eccentricity, e.

     I = moment of inertia of the weld about its

        mid-depth transverse axis.

     A = effective throat area of the weld.

     y = distance from the neutral axis of the weld

        length to its extremity.

The combined, effective maximum stress used in design is given by,

$$q_{max} = \sqrt{\sigma^2 + \tau^2} \tag{2.3}$$

The computed stress, q_{max}, is then compared to the allowable stress on the throat area and the weld leg size adjusted as necessary.

The following example is used to illustrate some of the variations of the basic method described above that are commonly in use at the present time.

2.2 Design Example

A fillet weld is required to connect a bracket to a column flange. The arrangement and loading are as shown in Fig. 2.1.

Method 1[7] (Weld Considered as an Elastic Beam Element)

The weld is subjected to a direct shear force, P, and a moment,

$$M = P \times e$$

The moment of inertia of the weld about the centroidal axis of the weld configuration can be conveniently calculated on the basis of unit widths of weld;

$$I = \frac{2 \times 1 \times 6^3}{12} = 36.0 \text{ in.}^4$$

and,

$$M = 8 \times 6 = 48.0 \text{ in.-kips.}$$

Direct shear stress, $\tau = 8/12 = 0.67$ k/in.

Bending shear stress, $\sigma = \frac{48 \times 3}{36} = 4.0$ k/in.

Combining these stresses vectorially yields,

$$q_{max} = \sqrt{\tau^2 + \sigma^2} = 4.05 \text{ k/in.}$$

The allowable stress on welds formed from E60 electrodes[10] is 0.8 k/inch per 16th inch of leg size.[1]

Therefore required leg size = $\dfrac{4.05}{0.8}$ = 5 (sixteenths) inch.

Method 2[17] (Bearing Area of Plates Considered)

This method considers the bearing of the plates below the neutral axis. An elastic analysis is used which is based on the moment of inertia of the throat area of the welds above the neutral axis and the plate bearing area below the neutral axis. The same illustrative problem as used in Method 1 is used to illustrate the analysis.

Referring to Fig. 2.2, the location of the neutral axis, $\bar{y}$, is determined by taking the moments of the shaded areas about the neutral axis. Assume a weld leg size, (t) of 3/8 inch.

From the relationship that the moment of plate bearing area must equal the moment of weld area;

$$\frac{1}{2} \times \frac{\bar{y}^2}{2} = 2 \times .707 \times \frac{3}{8} \times \frac{(6 - \bar{y})^2}{2}$$

from which,

$$\bar{y} = 3.2 \text{ inches.}$$

and,

$$I = \frac{1}{2} \times \frac{(3.2)^3}{3} + 2 \times .707 \times \frac{3}{8} \times \frac{(2.8)^3}{3} = 9.33 \text{ in.}^4$$

Now,

$$\text{stress due to bending, } \sigma_{max} = \frac{P \times e \times (6-\bar{y})}{I}$$

$$= \frac{8 \times 6 \times 2.8}{9.33}$$

$$= 14.4 \text{ (ksi)}$$

and the direct shear stress, $\tau = \dfrac{P}{A}$

$$= \frac{8}{12 \times .707 \times .375}$$

$$= 2.52 \text{ (ksi)}$$

From which,

$$q_{max} = \sqrt{\sigma^2 + \tau^2}$$

$$= \sqrt{(14.4)^2 + (2.5)^2}$$

$$= 14.7 \text{ (ksi)}$$

$$\text{Allowable stress} = \frac{0.8 \times 6 \times 8}{.707 \times 3}$$

$$= 18.2 \ (ksi)$$

Therefore the 3/8 inch weld is adequate.

These two methods summarise the present design procedures commonly used to analyse and design fillet welds that are subjected to combined bending and shear stresses when the weld in the compression zone is not free to deform. The following points may be noted with regard to these current methods:

1. It has been clearly demonstrated [6,20] that both the strength and deformation of an element of a fillet weld depend on the angle of resisting force to which that element is subjected. Neither of the above methods recognises this property of fillet welds.

2. Both methods are based on the assumption that the load - deformation response of the weld is linear and that the proportional limit is not exceeded. However, recent research has shown that the assumption of a linear response is not correct and that it is very difficult to define a proportional limit for welds. [5,19]

3. Although Method 2 is probably a more rational approach to the problem, it unjustifiably assumes that the stress-strain properties of both the weld metal and the base metal are

identical in nature.

4. Since the weld is, in each case, considered to be an elastic beam element it is not valid to assume that the maximum combination of bending and shear stresses occurs at the extreme fibre of the weld.[19] As determined by elementary beam theory, the maximum bending stress occurs at the extreme tension or compression fibre whereas the maximum shear stress occurs at the location of the neutral axis of the cross-section.

2.3 Review of Previous Research

Very few previous researchers in this field have given any consideration to the variation of fillet weld strength as related to the angle of applied load. However, several researchers have done tests on side fillet welds and end fillet welds.[3,6] These tests have shown that transverse fillet welds are approximately 30 to 35 per cent stronger than longitudinal fillet welds.

In 1939, Vandeperre and Joukoff[20] conducted a series of tests on the strength of fillet welds as a function of the angle between weld and load. From these tests it was concluded that the maximum throat stress for inclined fillets is intermediate between the values for longitudinal and

transverse fillets. In that instance, however, a relationship for weld strength as a function of load angle was not presented.

In 1935 Schreiner[18] carried out a series of tests on fillet welds subjected to bending with shear. Only large ratios of eccentricity of load to weld length were considered in these tests. The results showed that the present design methods are very conservative and give a factor of safety in the order of 5 when based on the ultimate strength of the weld and related to present allowable stresses specified for fillet welds.[1]

In 1959 Archer, Fischer and Kitchen[3] reported a series of tests which considered the combined effects of shear force and bending moment on two parallel fillet welds used in the attachment of a bracket to a column. The ratio of eccentricity to weld length in these tests varied from 0.0 to 1.3. These investigators concluded that the present working stress method of design yields a factor of safety which varies with the ratio of eccentricity to weld length, (e/L), from 3.6 to as high as 7.6. (The recent increase in allowable weld stresses[1] puts this range in the order of 2.7 to 5.7). Again, these investigators did not consider the effect of the variation in strength of an element of weld with the angle of applied load.

In 1965, Fisher[13] proposed a general mathematical expression for the load - deformation response of high-strength bolts loaded in shear. In 1969 Butler and Kulak,[6] presented a modification of this expression suitable for the analysis of fillet welds subjected to shear. This expression considers the load - deformation response of elemental lengths of fillet weld under different angles of loading. In particular, the expressions developed were for 1/4 inch fillet welds made with E60 electrodes.[10] These expressions have been adopted for analytical purposes in this investigation and they are presented in detail in Chapter III of this report.

On the basis of this literature review, the following critical points have arisen:

1. In the current method of design, the factor of safety is known to vary over a wide range as the ratio of eccentricity to weld length varies.[3,18] Archer, Fischer and Kitchen reported low factors of safety (in the order of 3.6) for low ratios of eccentricity to weld length (in the order of .06) and high factors of safety (about 7.6) for high ratios of eccentricity to weld length (about 0.46). This high variability of the factor of safety makes the present criterion for design highly unsatisfactory.

2. The variation of the strength of an elemental length of fillet weld with angle of load is not considered in

present design stress provisions. The strength of a transversely loaded fillet weld is about 30 per cent greater than that of an axially loaded fillet weld.[6,20]

3. As pointed out by Archer, Fischer and Kitchen[3]; "The design of fillet welds in all situations appears to have been based on the methods used for riveted joints." This is not necessarily a justifiable approach to the design of fillet welds.

4. The present design approach is based on the assumption of completely elastic behaviour of the weld. The ordinary equations of elastic analysis are used to determine the stresses in the weld and since this is known to be not strictly applicable, a high factor of safety is used. Several previous investigators have attempted to modify the existing elastic analysis equations and apply them to the analysis of fillet welds in order to reduce the factor of safety. However, this has not proven to be satisfactory since the resulting factor of safety varies over a wide range depending on the ratio of eccentricity to weld length.

An examination of the available literature reveals that no investigator has attempted to analyse eccentrically-loaded fillet welded connections when the ultimate capacity of the weld has been reached and the weld is not free to rotate in the compression zone. However, some investigators[3,14] have modified the presently available elastic analysis formulas

in an effort to approximate ultimate capacities of such connections. In such cases, the factor of safety becomes more uniform but only for a small range of the ratio of eccentricity of load to fillet weld length.

In all cases, no consideration has been given to the true load - deformation response of the weld. Present design procedures employ a theoretical analysis which is not strictly applicable. This results in very conservative factors of safety.
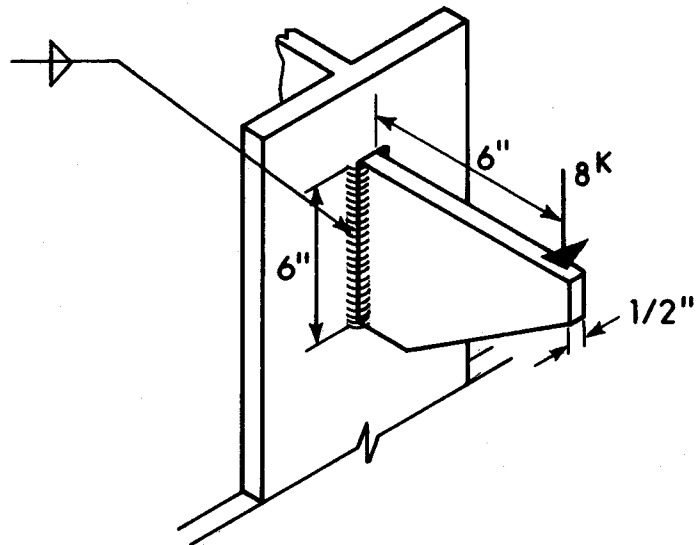
FIG. 2.1 WELDED SUPPORT BRACKET
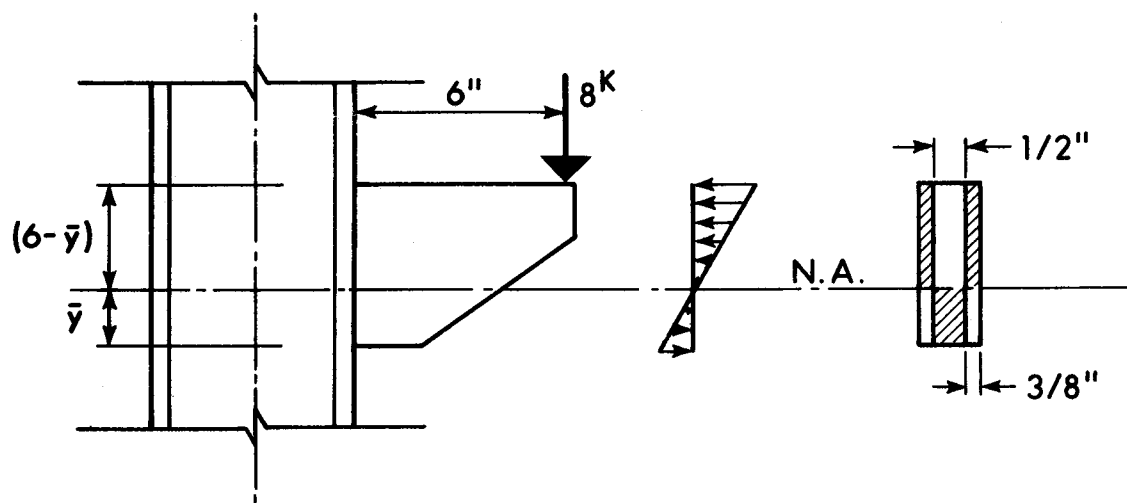
FIG. 2.2 DESIGN EXAMPLE (METHOD 2)

3. A N A L Y T I C A L   S T U D I E S

3.1 Introduction

The analytical method developed herein predicts the ultimate capacity of an eccentrically loaded fillet welded connection such as the one shown in Fig. 3.1. As has been pointed out, the weld is not free to deform in the compression zone when subjected to a rotational deformation. The method is based on a recognition of the load - deformation response of individual weld elements and it assumes that a continuous line of weld can be broken down into a series of these individual elements. The method has already been successfully used to analyse eccentrically loaded fillet welded connections in which the weld is free to deform in both the tension and compression zones of the connection.[5] Originally, this theoretical approach was developed for the prediction of the ultimate capacity of eccentrically loaded bolted connections.[12,13]

In this analysis a continuous line of weld is considered to be a series of individual weld element fasteners. Each weld element is considered to be a separate fastener with a characteristic load - deformation response depending on the angle between it and the load which it resists. It is

20

assumed that this load acts through the center of gravity of the element. The overall resisting capacity of the continuous line of weld is obtained by summing the individual resisting capacities.

Empirical relationships for the load - deformation response of individual weld elements have been developed by Butler and Kulak.[6] These empirical relationships incorporate the effect of different angles of loading with respect to the weld elements. The necessary parameters for correlating the present test specimens were obtained from weld coupons tested at zero angle of load to weld. The adjusted values of ultimate load and ultimate deformation were then substituted into the empirical relationships. These relationships are presented in Sections 3.2.2 and 3.2.3

3.2 Prediction of Ultimate Strength

3.2.1 Assumptions

In predicting the ultimate capacities of the full-size connection specimens the following assumptions are made:

1. The ultimate capacity of a connection is reached when a critical weld element has reached its ultimate deformation. For most

cases, this will be the weld element farthest from the instantaneous center of rotation.

2. The load-induced resisting force of each weld element acts through the center of gravity of that element.

3. The deformation of each weld element varies linearly with its distance from the instantaneous center and takes place in a direction perpendicular to its radius of rotation.

4. The connecting plates in the compression zone of the connection are in direct bearing at the time that the ultimate load is reached.

3.2.2 Load - Deformation Response of Weld Elements

The prediction of the ultimate capacities of full-size eccentrically loaded welded connections will be based on the load - deformation response of individual weld elements. This load - deformation response can be expressed by the following relationship:

$$R = R_{ult} (1 - e^{-\mu\Delta})^{\lambda} \qquad\qquad 3.1$$

where,

R = weld element load at any deformation.

R_{ult} = ultimate load attainable by the weld element at any given angle of loading.

Δ = deformation of the weld element due to the combined effect of shearing, bending, and bearing stresses as well as local bearing deformations in the connecting plates.

μ, λ = experimentally determined regression coefficients.

e = base of the natural logarithm.

The load - deformation response of an individual weld element depends on the angle at which the weld element is loaded with respect to its longitudinal axis.[6] Therefore the values of the constants, R_{ult}, μ, and λ in equation 3.1 will be different for different values of this angle. The empirical relationships for these constants as functions of the angle of load, θ, have been established by Butler and Kulak.[6] These relationships were obtained for a weld element fastener approximately 1 inch long having a nominal leg size of ¼ inch and formed with E60 electrodes[10] on a base metal of ASTM - A36 steel.[2]

For the full-size connections used in this experiment the angle of resisting load to the weld element axis can be any value between 0 and 90 degrees. The angle that a resisting force makes with a particular weld element can be determined from the co-ordinates of the center of the weld

element using the instantaneous center of rotation of forces as the origin.

3.2.3 Development of Theory

In Fig. 3.2(a) a load, P, is shown to act at an eccentricity, e, from a continuous line of fillet weld of length, W_1. In the analysis of this type of connection the weld length in the tension zone is subdivided into a number of equal length weld elements. Each weld element is then considered to be a single fastener in a line of fasteners having unique load - deformation properties depending on the angle of load to which an element is subjected.

In order to determine the angle of load acting on a weld fastener element, the location of the instantaneous center of rotation of the weld element forces must be determined. Initially, trial locations for the position of both the neutral axis and the instantaneous center are chosen. The instantaneous center must lie on the neutral axis and be on the side of the weld opposite from the load. As shown in Fig. 3.2(a), r_o is the distance between the instantaneous center and the longitudinal axis of the line of weld. The distance of the neutral axis from the extreme compression fibre is termed y_o. The location of the center of gravity of

each weld element is established by x- and y- co-ordinates with respect to the instantaneous center as the origin of co-ordinates.

The radius of rotation, r_i, for the ith weld element is given by:

$$r_i = \sqrt{r_o^2 + y_i^2} \qquad\qquad 3.2$$

Since the resisting force on any element is assumed to act perpendicular to the radius of rotation, the angle of inclination of the force with respect to the weld element axis is described by:

$$\tan \theta_i = \frac{y_i}{r_o} \qquad\qquad 3.3$$

The maximum deformation in the line of weld will occur at the nth weld element located furthest from the instantaneous center. It is determined by the empirical equation,[6]

$$\Delta_{max} = 0.225 \, (\theta_n + 5)^{-0.47} \qquad\qquad 3.4$$

where θ_n is in degrees.

Since the deformation of each weld element is assumed to vary linearly with its distance from the instantaneous center, the deformation of the ith weld element is given by,

$$\Delta_i = \frac{r_i}{r_n} \Delta_{max} \qquad\qquad 3.5$$

The magnitude of the force on any element can now be obtained from equation 3.1.

As previously described, R_{ult}, μ, and λ now depend upon the value of the corresponding angle, θ. The required relationships have been established[6] as:

$$R_{ult_i} = \frac{10 + \theta_i}{0.92 + .0603\theta_i} \qquad\qquad 3.6$$

$$\mu_i = 75\ e^{.0114\theta_i} \qquad\qquad 3.7$$

$$\lambda_i = 0.4\ e^{.0146\theta_i} \qquad\qquad 3.8$$

These empirical relationships were developed for ¼ inch fillet welds.[6] The value of R_{ult} is in terms of force per unit length and its value is assumed to vary linearly with leg size and can be modified accordingly.

Each weld element is now described as resisting a force, R_i, which has vertical and horizontal force components given by,

$$(R_i)_v = \frac{r_o}{r_i} \times R_i \qquad\qquad 3.9$$

and

$$(R_i)_h = \frac{y_i}{r_i} \times R_i \qquad\qquad 3.10$$

Referring to Fig. 3.2(b), it will here be assumed that stress distribution of the plates in bearing in the compression zone below the neutral axis is triangular with a maximum ordinate equal to the yield point of the plate material. The resultant horizontal force of this stress distribution is therefore located a distance two-thirds y_o below the neutral axis. (Other assumed stress distributions for the bearing of the plates in the compression zone have been investigated and these will be discussed later).

The length of the weld in the compression zone below the neutral axis is assumed to resist a vertical component of force only. Taking δ to be the vertical component of deformation in each weld element in the tension zone and referring

to Fig. 3.2(a),

$$\delta = \frac{r_o}{r_i} \times \Delta_i \qquad\qquad 3.11$$

Substituting the value of Δ_i from equation 3.5 this becomes,

$$\delta = \frac{r_o}{r_n}\left(\Delta_n\right) \Delta_{max} \qquad\qquad 3.12$$

From equation 3.12 it is seen that δ has a constant value. Therefore, according to this analysis, the weld has a uniform vertical deformation over its whole length. The vertical shear force, V_b, resisted by the length of weld below the neutral axis can therefore be expressed by,

$$V_b = \frac{y_o}{(W_1 - y_o)} \times \sum_{1}^{n} (R_i)_v \qquad\qquad 3.13$$

The resultant force of the triangular stress distribution shown in Fig. 3.2(b) acts two-thirds y_o below the neutral axis. H_b is the resultant of the stress block shown and is given by:

$$H_b = \frac{y_o \, \sigma_y \, t}{2} \qquad\qquad 3.14$$

where σ_y is the yield stress of the plate material and t is the plate thickness.

The known quantities in this analysis are the length of weld, W_1, the thickness, t, of the connected plate, the eccentricity, e, of the load, the yield stress, σ_y, of the plate, the average leg size of the weld, and the length, E_1, of each weld element. The unknowns are the ultimate load, P, of the connection, the location of the neutral axis from the extreme compression fibre, y_o, and r_o, the location of the instantaneous center along the neutral axis.

In the analytical procedure, initial values are assumed for r_o and y_o. All the forces, R_i, in the weld elements are thereby defined as are the vertical shear force, V_b, of the weld and the bearing force, H_b, of the plates in the compression zone. In order that the connection be in equilibrium the equations of statics must be satisfied:

$$\Sigma F_x = 0 \qquad \qquad 3.15$$

$$\Sigma F_y = 0 \qquad \qquad 3.16$$

$$\Sigma M = 0 \qquad \qquad 3.17$$

Taking the sum of the moments of all the forces about the instantaneous center, equation 3.17 becomes:

$$P(e+r_o) - \sum_1^n (R_i r_i) - r_o V_b - (2/3) y_o H_b = 0 \qquad 3.18$$

The sum of the vertical forces on the connection yields:

$$\sum_1^n (R_i)_v + V_b - P = 0 \qquad 3.19$$

From equations 3.18 and 3.19 expressions for P are obtained. Subtracting these gives an equation in which the only unknowns are y_o and r_o, namely:

$$\sum_1^n (R_i)_v + V_b - \left[\sum_1^n (R_i r_i) + r_o V_b + (2/3) y_o H_b / (e+r_o) \right] = 0 \qquad 3.20$$

Summing the forces in the x- direction gives:

$$H_b - \sum_1^n (R_i)_h = 0 \qquad 3.21$$

The initial trial value of y_o is used in equation 3.20 and successive values of r_o are chosen by an iterative technique until the equation is satisfied. The pair of values, r_o and y_o, which satisfy this equation are then used to evaluate the terms in equation 3.21. If this equation is also satisfied the ultimate load has been obtained and is that given by equation 3.19. If equation 3.21 is not satisfied

by this pair of values, then another value for y_o is chosen
and the procedure is repeated.

This iterative procedure requires numerous cal-
culations and is generally too laborious for hand com-
putation. A digital computer program has been written to
perform the calculations and is given in the Appendix.
The program has been written in Fortran IV language and is
suitable for the IBM 360 computer. The program generates
successive approximations for y_o and r_o by using the Reguli
Falsi iterative technique.[11] Pairs of values of r_o and
y_o are successively generated until equation 3.20 is
satisfied to the extent that the load, P, is within ±1% of
its true value and y_o is within ±1% of its true value.

The procedure outlined above has been extended
to predict the ultimate capacities of a series of full-
size test connections of various weld configurations.
These connections were tested to ultimate in order to
verify and to justify the use of this procedure in pre-
dicting the ultimate loads for a full range of this type
of eccentrically loaded connections. These topics are
discussed in Chapters V and VI.
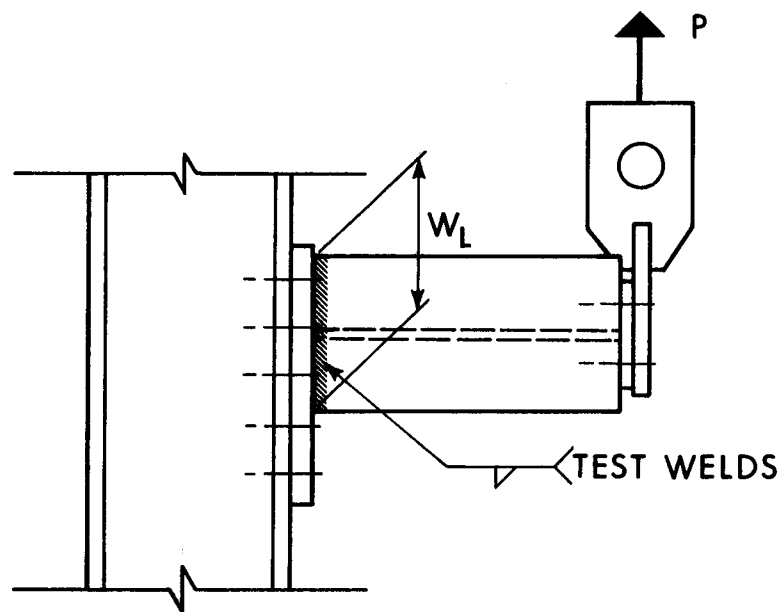
FIG. 3.1 ECCENTRICALLY LOADED TEST SPECIMEN (SERIES ONE)

a.

b.
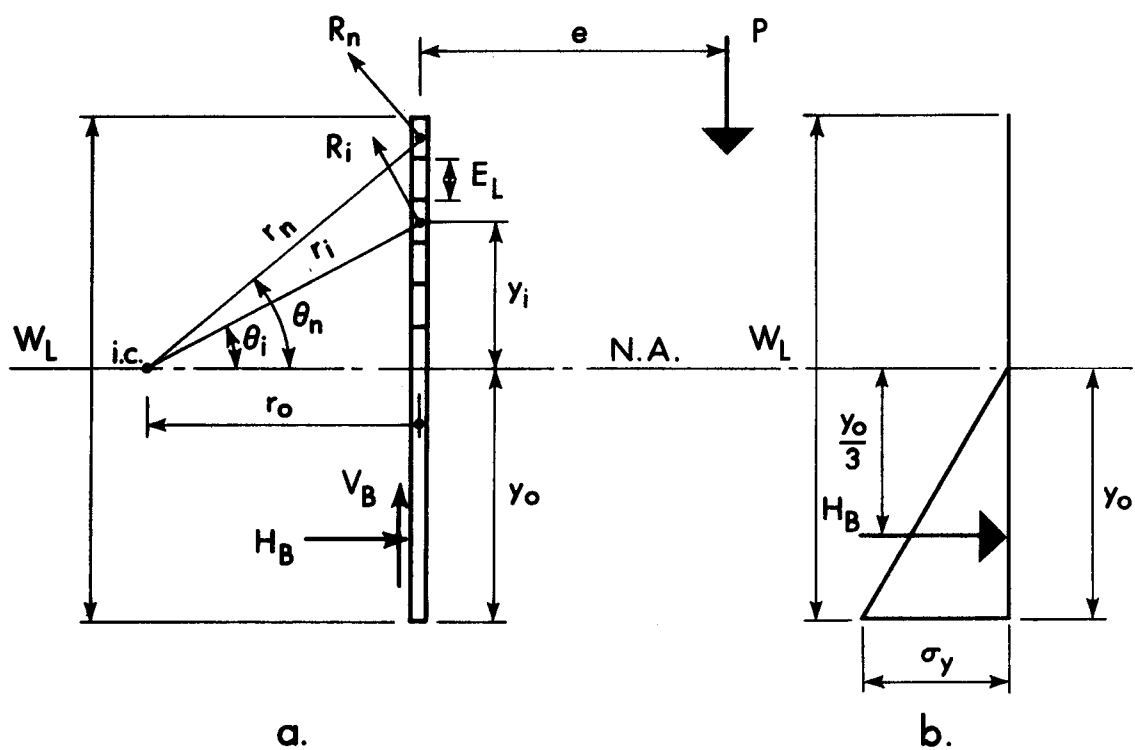
FIG. 3.2 ECCENTRICALLY LOADED FILLET WELD

4. E X P E R I M E N T A L   P R O G R A M

4.1 Scope

The experimental portion of this program consisted
of three series of tests on full-size specimens. Test Series
One was set up to verify the analytical technique outlined
in Chapter III. For this purpose, the simplest weld config-
uration, namely, a vertical line of fillet weld, was chosen.
There was good correlation between test and theory in this
series and it was decided to expand the analytical and
experimental program to include two other weld configurations,
a T-shaped weld and an I-shaped weld. The basic similarity
among these three series of eccentrically loaded connections
was the suppression of rotational deformation of the weld in
the compression zone due to direct plate bearing.

The first series of tests consisted of eight speci-
mens designed to simulate a plate-to-column-flange welded
connection eccentrically loaded in a direction parallel to
the line of fillet weld. Such a connection could be made
at the junction of a beam web and column flange, for example.
The second test series consisted of four specimens designed
to simulate a T-shaped fillet weld connecting the web and tension

33

flange of a beam in a beam-to-column connection. These specimens were also eccentrically loaded perpendicular to the flanges in the plane of the web. The third series of tests were identical to the second series except that the weld configuration included a fillet weld across the beam flange in the compression zone.

Each of these series of tests was accompanied by five weld coupon tests and a series of tensile coupon tests on the base metal. The weld coupon tests were designed so that the ultimate load of a longitudinal fillet weld, with characteristics as close as possible to the weld in the full-size pieces, could be obtained. The tensile coupons were tested to obtain the yield stress level of the base metal. In all cases the specimens were designed so that the welds were the critical component. All steel used in the connections was ASTM - A36[2] and all test welds had a nominal leg size of ¼ inch, and were formed using AWS E60[10] electrodes. In order to ensure a fillet weld as uniform as possible, it was specified that all welding be performed by the same weldor using electrodes from the same lot. Weld returns were later removed ensuring lengths of weld reasonably uniform throughout.

4.2 Specimen Details

4.2.1 Test Series One

Each test specimen of this series consisted of a wide flange section with a ½ inch load plate welded to one end as shown in Fig. 4.1. The other end of the specimen was attached to a 3/4 inch reaction plate by one line of fillet weld along the outer side of each flange. These were the test welds and before their deposition the wide flange section was made flush and square with the plate. Interaction of the web in bearing with the base plate was prevented by cutting back the web 1 inch from the end of each of the sections.

Each specimen was attached to the flange of a stub column by bolting the reaction plate to the flange using high-strength bolts. The specimens were oriented on the column so that the load applied by a hydraulic jack acting in tension induced bending about the weak axis of the wide flange section.

The variables in this series of tests were the length of fillet weld, the eccentricity of load and the thickness of the connected plate. As shown in Table 4.1 the nominal weld length remained constant at 8 inches for specimens

A-1 to A-6 while the eccentricity and plate thickness were varied. For specimens A-7 and A-8 the weld length was nominally 12 inches, and the plate thickness remained constant while the eccentricity of load was varied. The fillet weld leg dimension for each specimen, as given in Table 4.1, is the average of 36 individual measurements covering both lines of fillet weld. In the case of specimen A-6 the flanges of a 10WF66 section were cut back 2 inches from each edge to form a symmetrical section having 8 inch flanges.

4.2.2 Test Series Two

This series of tests consisted of four full-size connections having a T-shaped test weld configuration. Each specimen was made of a wide-flange section with a ½-inch load plate attached to one end as shown in Fig. 4.2. A 1-inch reaction plate was attached to the other end of the wide-flange section by means of the test welds. The test weld consisted of a line of fillet weld on the outside edge of one flange only, and a line of fillet weld on either side of the web of the section. The flange weld extended across the full width of the flanges and the web welds extended the full depth between the web fillets. Before the test welds

were deposited the wide flange section at the test weld end was fitted flush and square with the reaction plate.

In fabricating these specimens, there was difficulty in devising a means for obtaining a uniform length of weld along the webs of these sections at the test weld end. However, it was felt that the exact length of this weld would not be too critical since calculations showed that most of the capacity of the specimen was developed by the weld along the tension flange.

As shown in Table 4.2, the variables in this series of tests were the length of the web welds, the eccentricity of load, the flange area, and the web area. The fillet weld along the flange of each specimen was equal to the flange width. For all four specimens the fillet weld along the tension flange was maintained at a nominal length of 4 inches. The only difference between specimens B-1 and B-2 was a change in eccentricity from 15 inches to 20 inches. For specimens B-3 and B-4 the eccentricities were also 15 inches and 20 inches, but in this case a different wide-flange section was used. Therefore specimens B-3 and B-4 differed from B-1 and B-2, respectively, by a change in the flange and web areas and a change in the length of the web fillet weld. The fillet weld leg dimension shown in Table 4.2 for each length of weld is the average of several individual leg size measurements.

During fabrication, the flange width of each of the four specimens was reduced to 4 inches while maintaining a symmetrical section at the test weld end of the section. For specimens B-1 and B-2, and B-3 and B-4, the flange corners were cut back at 9:12 and 12:12 slopes, respectively. The design of the specimens, requiring the test welds to be the critical component in each connection, was based on the plastic moment capacity of the reduced section.

4.2.3 Test Series Three

The four full-size test specimens used in this series of tests were identical to those used in Series Two except that both flanges were welded at the test weld end. The result of this was an I-shaped test weld configuration rather than a T-shaped one. All dimensions of these specimens were nominally the same as those of Series Two. The actual (average) dimensions are presented in Table 4.3.

For each type of wide-flange section used in the fabrication of the full-size test specimens, two tensile coupons were taken. These coupons were cut from the same length of section as used in the fabrication of the test specimens. Two coupons from each section were cut from diagonally opposite sides of the flanges. These coupons

were tested in a 200,000-pound capacity Baldwin Testing

Machine. The test results were used to obtain the static

yield point of the base metal.

4.2.4 Weld Coupons

For each of the three groups of full-size speci-

men tests, a series of five weld coupon tests was conducted.

As has been described earlier, the weld coupon tests are

required to establish the load - deformation response for

elemental lengths of fillet weld. The weld coupons, as shown

in Fig. 4.3, were loaded with the weld axis parallel to the

direction of applied load.

The test data from the weld coupons are presented

in Table 4.5. All coupons were fabricated from ASTM A36

steel plate[2] having a specified yield stress of 36 ksi.

All fillet welds were made with AWS-E60 electrodes[10]

taken from the same lot as used for the corresponding full-

size test pieces. It was also specified that the same

weldor prepare these coupons and the corresponding full-size

test pieces. For each specimen the cross-sectional areas of

the connected parts were designed so as to ensure that the

weld failed before rupture of the plates. The plate thick-

nesses were also limited by the required weld leg size, in

order to conform with the regulations set forth in present

building codes. All weld dimensions were taken as averages of several individual measurements.

4.3 Test Set-up

A typical test set-up for the full-size specimens is shown in Fig. 4.4. The hydraulic jack acts in tension and transfers the load through the bolted connection of the load plates to the end of the test specimen. The load is transfered from the jack through a load cell which was previously calibrated in terms of kips per unit of strain.

All test specimens were bolted to the flange of a 6-foot high stub column fabricated from a 12WF85 section. The column was attached to the laboratory strong-floor by means of a base plate 3 inches thick and prestressed steel anchor bolts. The hydraulic jack was suspended from an overhead distributing beam which had its longitudinal axis aligned parallel to the axis of the specimen. Before each test, the jack was moved along the distributing beam until its axis was carefully centered at the eccentricity required for the testing. Freedom of rotation was provided at the load end of each specimen by means of a pin-connection between the load cell and the load plate.

4.4 Test Procedure

4.4.1 Full-Size Test Specimens

The test specimens of the type used in Test Series
One were attached to the stub column so that the weld lines
were vertical and the load from the jack induced bending
about the weak axis of the wide flange section. One rotation
measuring device was attached to each specimen adjacent to
the test weld. A second rotation gage, at the same elevation
as the one on the specimen was attached to the stub column so
that the relative rotation of the beam with respect to the
column could be obtained. Eight dial gages were attached to
each specimen near the test weld. The locations of these
gages are indicated schematically in Fig. 4.5. One dial
gage at the end of either weld was used to obtain the local
horizontal deformation in the tension zone of the weld.
Dial gages mounted on either side of the web were used to
obtain vertical deformations in the welds. These two dial
gages were mounted on the base support on metal brackets
attached to the wide-flange section.

In the second series of tests, each specimen was
mounted on the stub column so that bending was induced about
the strong axis of the wide flange section. The test weld
on the flange of the section was subjected to tension and

shear. The opposite flange of the section was subjected only to compressive bearing stresses against the reaction plate.

Fig. 4.6 shows the arrangement of the dial gages used on the full-size specimens tested in this series. Dial gage measurements similar to those described above were made for rotation and weld deformation. The horizontal deformation of the flange weld in the tension zone was measured by a dial gage placed near either end of the weld.

The test welds in Series Three had an I-shape configuration. The specimens were mounted on the stub column so that bending took place about the strong axis of the sections. The tension flange weld was subjected to shear and tension while the weld on the compression flange was subjected only to shear. The dial gage arrangement was identical to that used in Test Series Two.

In all three series of tests, an initial load of about 10% of the predicted ultimate was applied to the specimen. This load was then removed and the procedure repeated several times in order to remove any slackness in the assembly prior to starting the test. During testing in the elastic range, the load was increased in steps of about 10 to 15% of the predicted ultimate load. Beyond this stage the load was increased until a half revolution occurred on the dial gage showing maximum rate of deformation in the tension weld. At the end of each load increment the load was maintained at a

constant level until all gages were read. This procedure was repeated up to failure load of each specimen.

4.4.2 Coupon Tests

The weld coupons and tensile coupons were also tested in the 200,000-pound capacity Baldwin Testing Machine. Two dial gages were attached to each weld coupon so that the average local deformation of the axially loaded weld could be recorded. The rate of loading was maintained at about 2500 pounds per minute. The deformation and load were recorded at 5-kip intervals of loading for the first 20 kips and thereafter at 10-kip intervals as deformations increased at a greater rate. During this yielding in the welds more closely spaced readings were recorded. The testing continued up to and beyond the point at which the ultimate capacity and the ultimate defor- mation of the welds were observed.

The tension coupons were tested in the same machine at a slow rate of loading. An extensometer attached to the neck of each coupon was attached to a stress-strain recorder. When the yield point of the specimen was reached the loading rate was decreased until the strain, as indicated by the stress- strain recorder, remained constant. This procedure was re- peated several times and the static yield point of the base metal was thus obtained.

4.5 Test Results

4.5.1 Full-Size Test Specimens

The test results of Series One, Two and Three are presented in Table 4.4. The table lists the ultimate loads obtained from the tests and the corresponding predicted loads as obtained by using the analytical procedure outlined in Chapter III. Also shown in this table is the per cent error in the predicted load as compared to the actual load obtained during testing. The current allowable loads given in the table are based on the theory of Method 1 as outlined in Chapter II. In calculating these values the most recent allowable weld stress values[1] were used. The factors of safety presented in the table are based on the current allowable loads and the corresponding ultimate loads obtained in the tests.

For Test Series One, Fig. 4.7 shows the load - rotation relationship for each specimen. Each load increment is plotted against the corresponding rotation of the specimen with respect to the stub column. Specimen A-4 was the first one tested and electrical rotation gages were used. These gages proved to be not sensitive enough for the purpose and consequently reliable rotation readings were not obtained. As a result, Fig. 4.7 does not show a load - rotation curve for this specimen.

For Test Series Two, the load - rotation curves are plotted in Fig. 4.8 and the curves are for test specimens B-1 to B-4 inclusively. Fig. 4.9 shows the load - rotation curves for the test specimens of Series Three. These curves are comparable to those of Test Series Two and are plotted to the same scale.

4.5.2 Weld Coupon Tests

Fig. 4.10 shows the load - deformation responses obtained from weld coupons tested in conjunction with Test Series One, Two and Three, respectively. Table 4.5 shows the actual dimensions of the test welds as well as the actual ultimate loads and ultimate deformations. Before plotting, these results were adjusted to an equivalent ¼ inch leg size. Hence, the results in Fig. 4.10 are for ¼ inch fillet welds loaded at zero angle of load and having characteristics similar to those of the welds used in fabricating the corresponding full-size test specimens. Each curve is the average of the results obtained from five weld coupon tests.

TABLE 4.1 SPECIMEN DATA FOR SERIES ONE

SPECIMEN NUMBER	TYPE OF SECTION	LOAD ECCENTRICITY (inches)	AVE. WELD LENGTH (inches)	AVE. LEG SIZE (inches)	PLATE THICKNESS (inches)	STATIC YIELD BASE METAL (ksi)
A-1	10WF39	8.0	7.77	.31	.52	43.3
A-2	10WF39	12.0	7.86	.31	.52	43.3
A-3	10WF39	16.0	7.87	.30	.52	41.9
A-4	10WF39	20.0	7.81	.30	.53	41.9
A-5	10WF33	16.0	7.84	.30	.43	38.1
A-6	10WF66	16.0	7.92	.32	.76	38.4
A-7	12WF65	15.0	11.86	.29	.62	39.3
A-8	12WF65	20.0	11.80	.31	.62	39.3

TABLE 4.2 SPECIMEN DATA FOR SERIES TWO

SPECIMEN NUMBER	TYPE OF SECTION	LOAD ECCENTRICITY	AVERAGE WELD DIMENSIONS				STATIC YIELD BASE METAL (ksi)
			TENSION WELD		WEB WELD		
			LENGTH (inches)	LEG (inches)	LENGTH (inches)	LEG (inches)	
B-1	6WF25	15.0	4.61	.28	5.52	.30	43.8
B-2	6WF25	20.0	4.57	.31	5.52	.30	43.8
B-3	8WF40	15.0	4.38	.31	7.10	.30	41.3
B-4	8WF40	20.0	4.47	.31	7.10	.30	41.3

TABLE 4.3 SPECIMEN DATA FOR SERIES THREE

SPECIMEN NUMBER	TYPE OF SECTION	LOAD ECCENTRICITY	AVERAGE WELD DIMENSIONS (inches)						STATIC YIELD BASE METAL (ksi)
			COMPRESSION WELD		TENSION WELD		WEB WELD		
			LENGTH	LEG	LENGTH	LEG	LENGTH	LEG	
C-1	6WF25	15.0	4.19	.29	4.29	.30	5.50	.31	43.6
C-2	6WF25	20.0	4.44	.29	4.43	.29	5.52	.29	43.6
C-3	8WF40	15.0	4.24	.31	4.21	.32	7.15	.27	39.1
C-4	8WF40	20.0	4.09	.26	4.19	.29	7.12	.32	39.1

TABLE 4.4 TEST RESULTS FOR SERIES ONE, TWO, AND THREE

SPECIMEN NUMBER	ULTIMATE LOADS (kips)		PER CENT ERROR	CURRENT ALLOWABLE LOAD (kips)	CURRENT FACTOR OF SAFETY
	TEST	PREDICTED			
A-1	62.5	52.6	-16.0	9.8	6.4
A-2	39.0	35.7	- 8.5	6.7	5.8
A-3	23.1	25.9	+12.1	4.9	4.7
A-4	19.5	20.7	+ 6.1	3.9	5.0
A-5	23.6	22.5	- 4.7	4.9	4.8
A-6	32.6	30.8	- 5.5	5.3	6.2
A-7	59.7	64.8	+ 8.5	11.5	5.2
A-8	49.6	49.7	+ 0.2	9.1	5.5
B-1	46.6	40.3	-13.5	5.8	8.0
B-2	37.8	31.4	-16.9	4.5	8.4
B-3	62.5	61.4	- 1.8	8.4	7.5
B-4	51.0	46.2	- 9.4	6.4	8.0
C-1	46.6	40.9	-12.2	8.8	5.3
C-2	38.4	31.7	-17.4	6.6	5.8
C-3	66.0	59.6	- 9.7	11.9	5.6
C-4	46.1	42.1	- 8.7	8.5	5.5

TABLE 4.5 WELD COUPON TEST DATA

| TEST SERIES NUMBER | SPECIMEN NUMBER | AVERAGE WELD SIZES | | ULTIMATE LOAD | ULTIMATE DEFORMATION |
| | | LENGTH | LEG | | |
		(inches)	(inches)	(kips/in.)	(inches)
1	1-1	1.07	.25	9.25	.065
	1-2	1.03	.27	9.34	.059
	1-3	1.01	.26	9.69	.046
	1-4	1.02	.26	10.89	.050
	1-5	1.01	.26	9.49	.055
2	2-1	1.00	.27	10.61	.070
	2-2	.99	.25	10.83	.078
	2-3	1.00	.25	10.58	.070
	2-4	1.00	.25	11.18	.050
	2-5	.99	.26	10.44	.060
3	3-1	1.01	.31	9.66	.105
	3-2	1.00	.29	9.56	.095
	3-3	.97	.28	9.95	.063
	3-4	1.02	.30	9.87	.092
	3-5	1.00	.30	9.72	.067
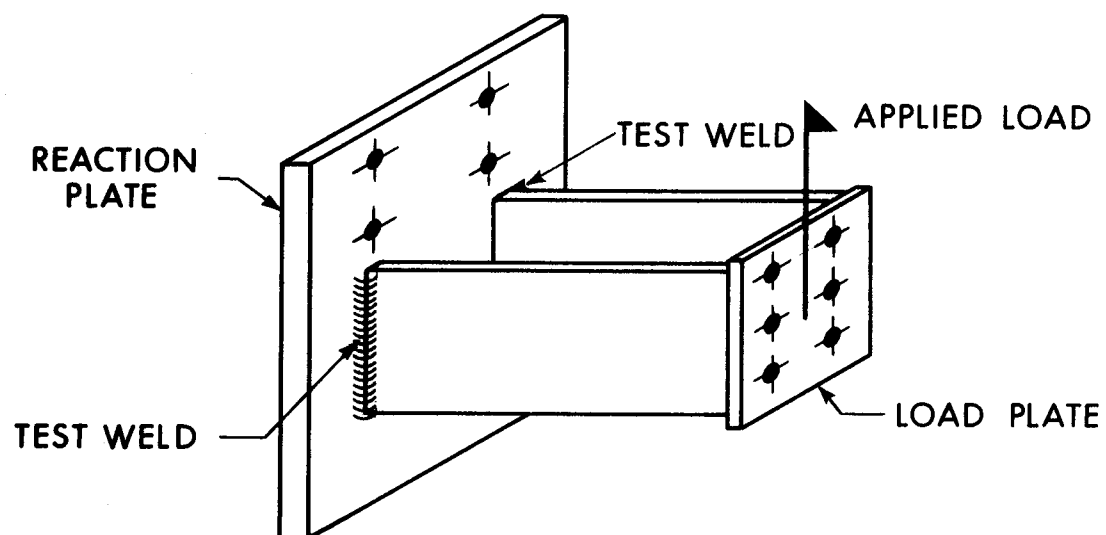
FIG. 4.1 TYPICAL TEST SPECIMEN (SERIES ONE)
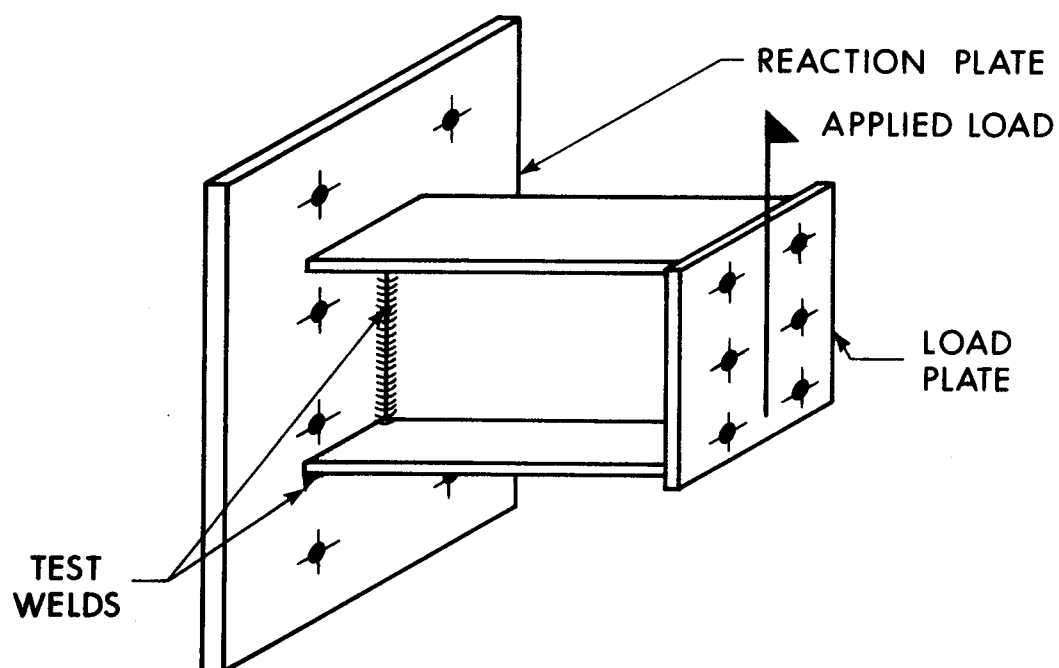
FIG. 4.2 TYPICAL TEST SPECIMEN (SERIES TWO)

$\frac{1}{4}"$ FILLET WELDS

$2\frac{1}{4}"$

$1\frac{1}{4}"$

TEST WELDS

WELD
LENGTH

$1"$

$\frac{1}{2}"$

$\frac{1}{2}"$
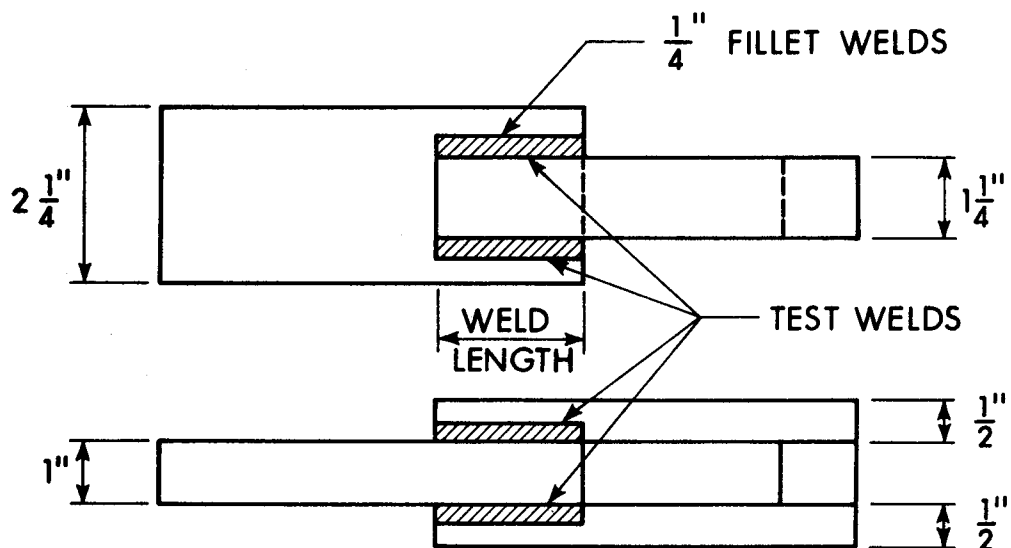
a. LONGITUDINAL WELD COUPON

DIAL GAGE

STEEL BRACKETS

SOLDERED
JOINTS
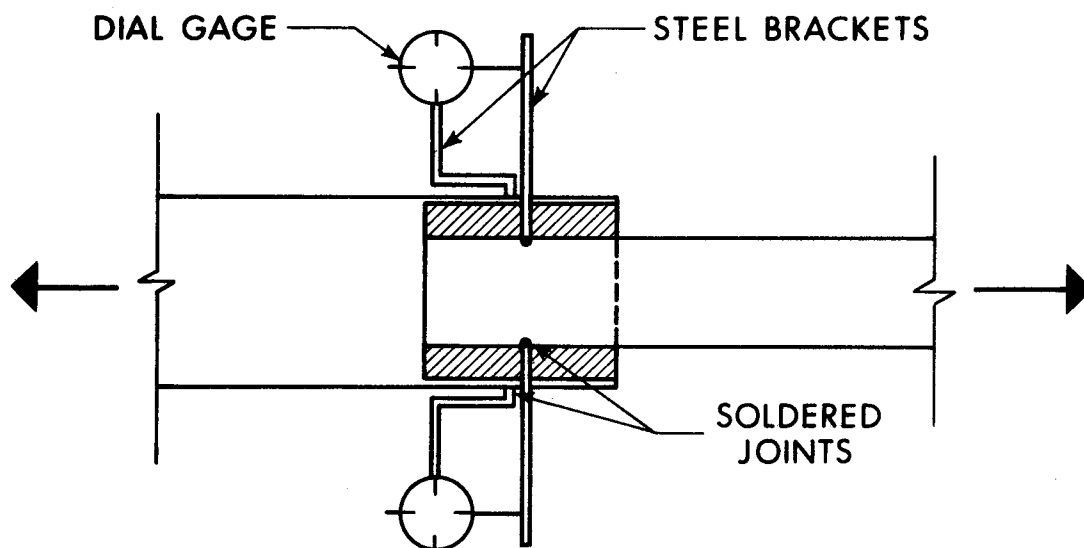
b. LOCATION OF DIAL GAGES

FIG. 4.3 TYPICAL WELD COUPON

HYDRAULIC JACK

LOAD CELL

STUB COLUMN

PIN CONNECTION

LOAD PLATE

TEST WELDS

REACTION PLATE

ANCHOR BOLT

COLUMN BASE

STRONG FLOOR

FIG. 4.4 TYPICAL TEST SET-UP

FIG. 4.5 LOCATION OF DIAL GAGES (SERIES ONE)

FIG. 4.6 LOCATION OF DIAL GAGES (SERIES TWO)
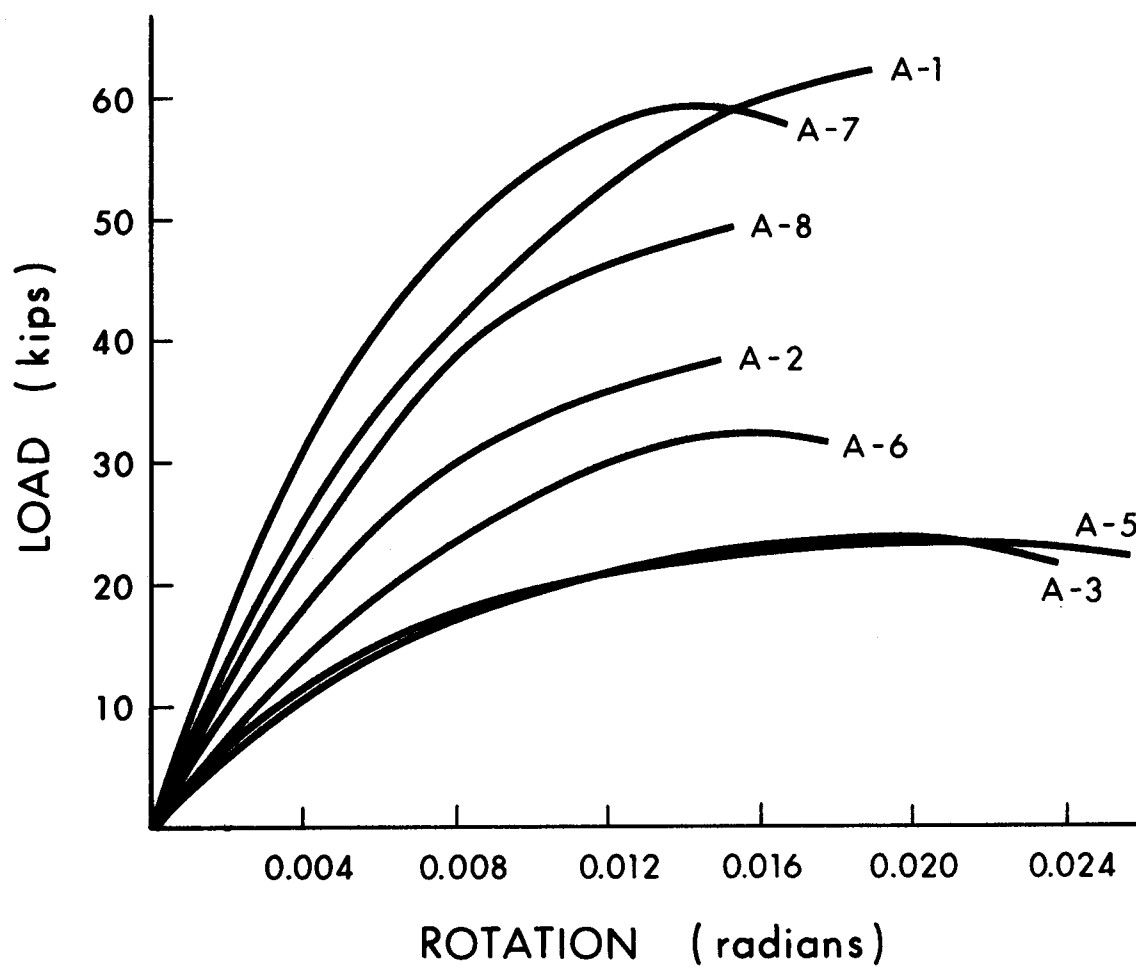
FIG. 4.7 LOAD-ROTATION (SERIES ONE)

FIG. 4.9 LOAD-ROTATION (SERIES THREE)

FIG. 4.8 LOAD-ROTATION (SERIES TWO)
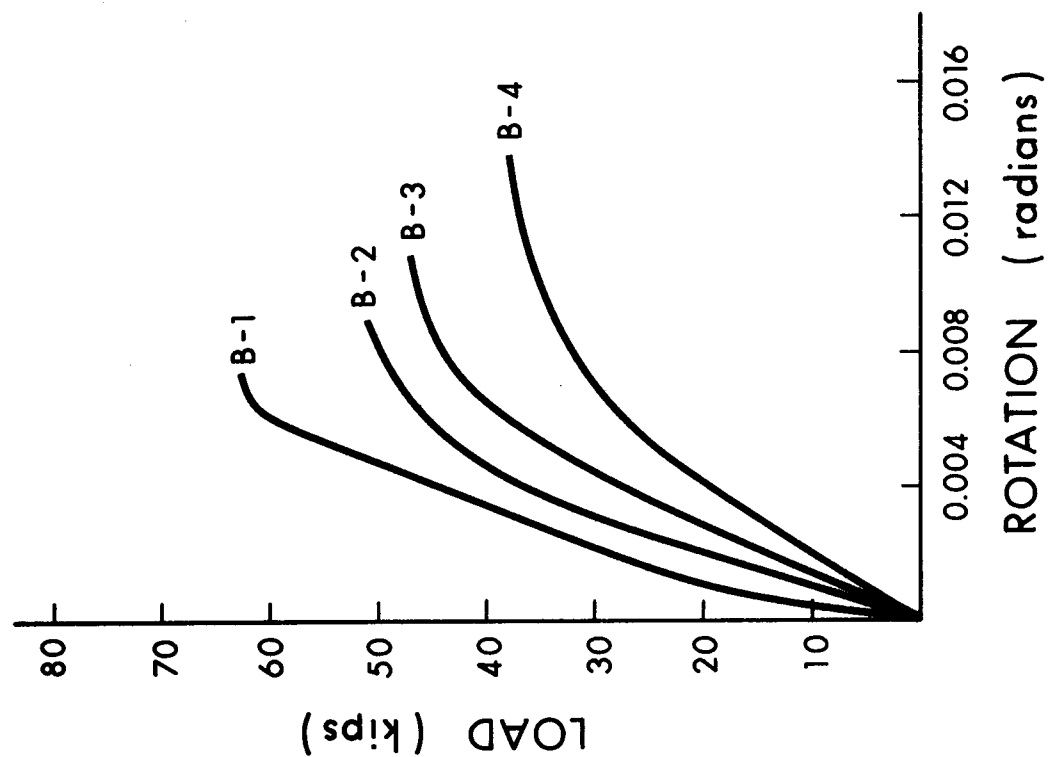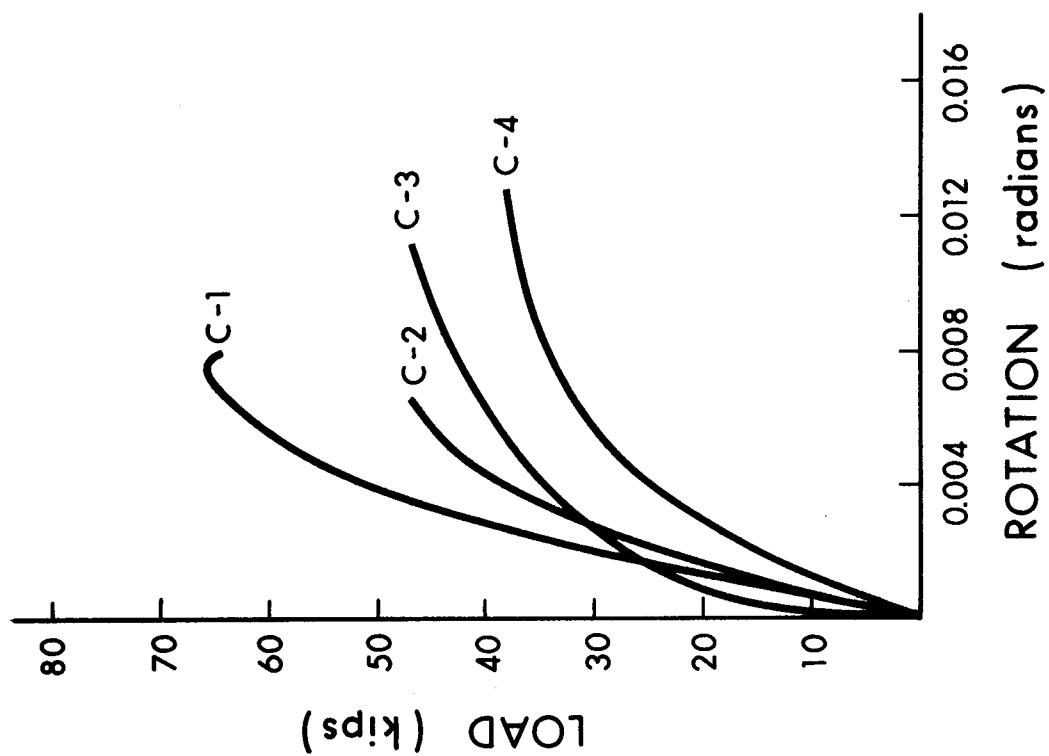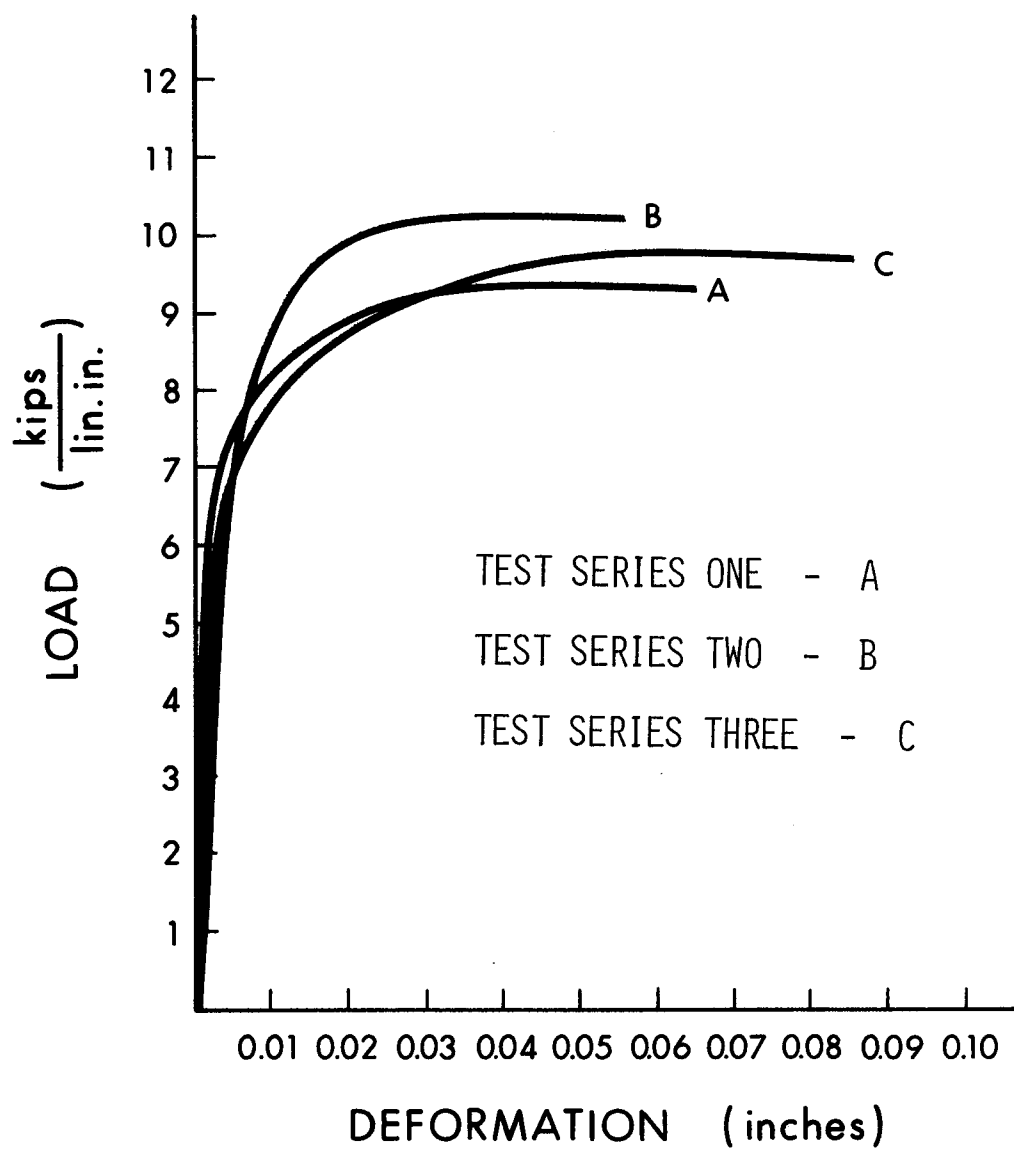
FIG. 4.10 LOAD-DEFORMATION CURVES: WELD ANGLE = 0°

5. DISCUSSION OF TEST RESULTS

5.1 Weld Coupon Tests

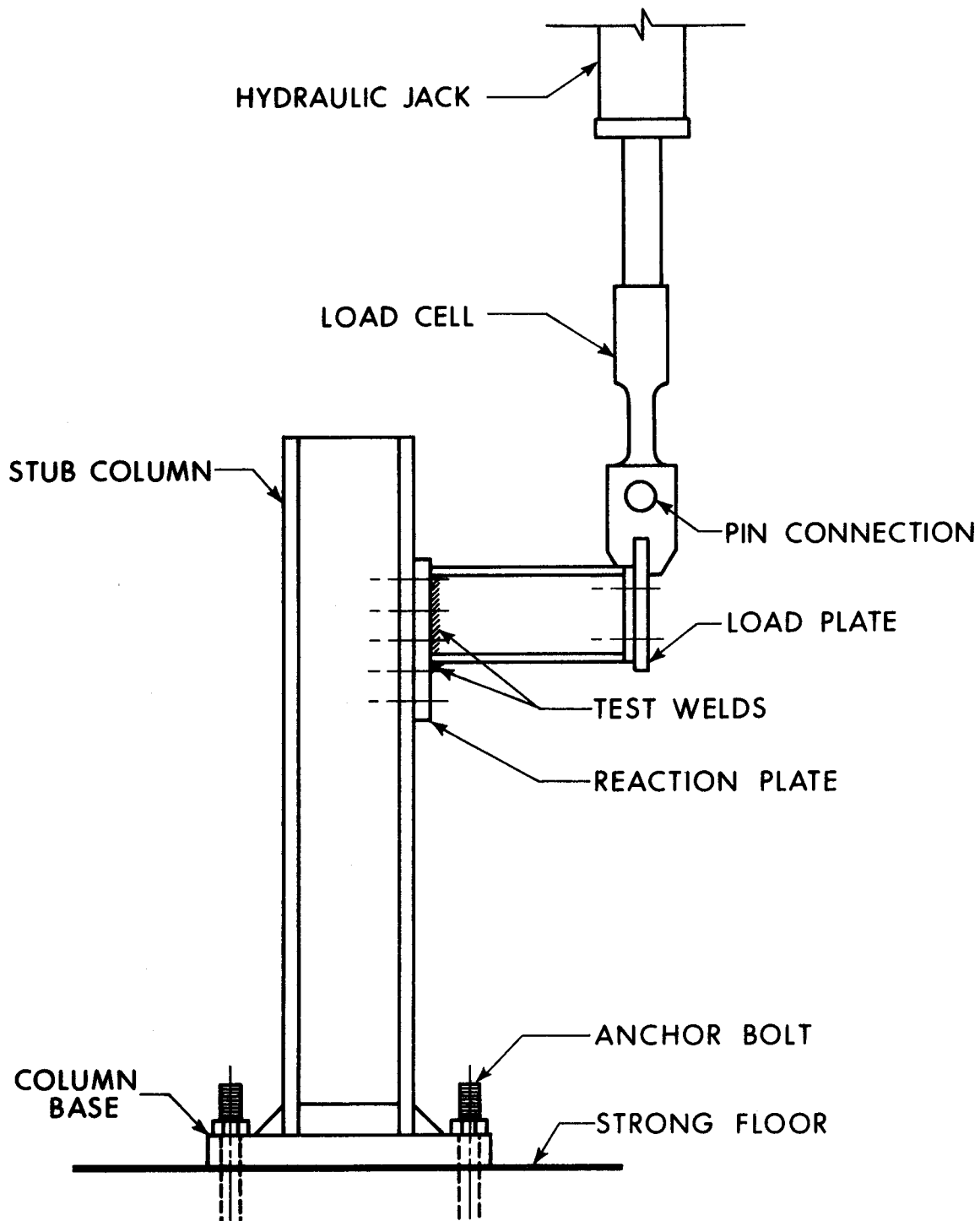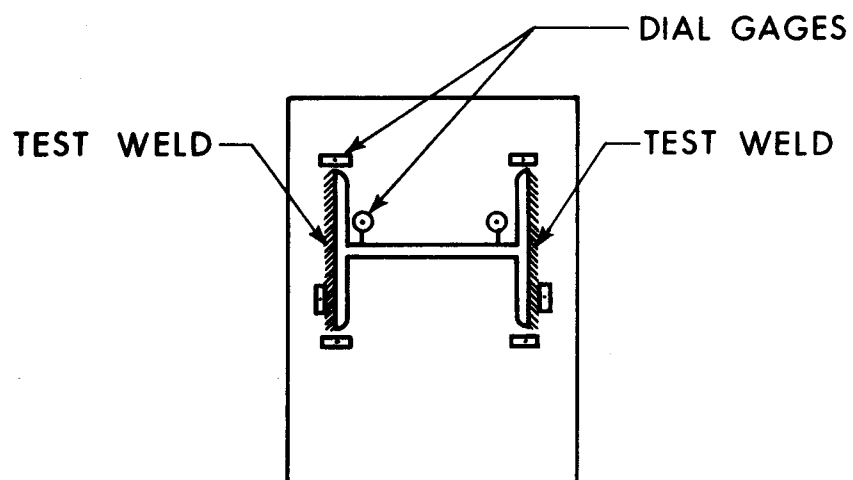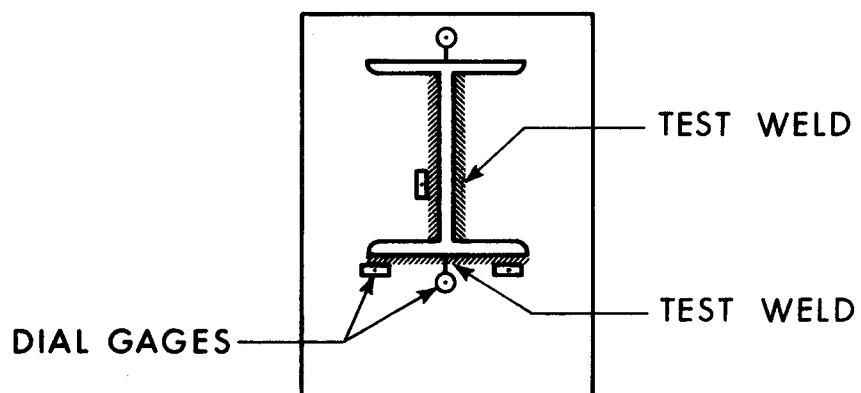The importance of the weld coupon tests in predicting the ultimate capacities of the full-size test specimens has already been pointed out. Any errors inherent in these results propagate throughout the mathematical analysis used to predict the ultimate capacities of the full-size test specimens.

The main sources of error in these tests were:

1. The inclusion of deformations other than that of the weld when measuring these deformations.

2. Non-axial loading due to non-uniform weld sizes.

3. Non-axial loading due to initial crookedness of the test specimen.

4. Measurements of weld leg sizes.

Ideally, the dial gages should be so placed as to measure only the weld deformation. However, the metal brackets holding the dial gages had to be attached to the base metal on

58

one side of the test weld and the brackets against which the dial gage rods rested, were attached to the other piece of base metal on the other side of the weld. Because of this, the dial gage measurements included local deformations of the base metal as well as deformations in the welds. It is assumed, however, that local deformation of the base metal is small compared to the deformation in the weld. In any event, it has been observed in the mathematical analysis that a small variation in the ultimate deformation of a weld does not seriously alter the value of the predicted ultimate load of the full-size specimens.

In fabricating a weld coupon, four separate elements of weld connecting the base metal pieces were located symmetrically about the longitudinal axis of the specimen. Thus, each weld element could be axially loaded only if all four elements had exactly the same dimensions. It was difficult, however, to maintain the required uniformity of weld and as a result the weld elements on a given coupon differed in size. Consequently, in most cases, the axial load from the main tension member was not distributed evenly among the four weld elements. The smallest weld element reaches its ultimate capacity first, thus inducing secondary stresses in the other welds. This results in an error caused by weakening and premature failure of the overall weld coupon connection.

Initial crookedness was noticeable in some of the weld coupons although not to a very great extent. This was most likely the result of cooling stresses set up in the welds in spite of proper sequence of weld deposition. In such cases, the applied axial load was not distributed equally among the separate weld elements. This again leads to secondary stresses in the welds and results in error due to premature failure of the overall weld coupon connection.

Weld leg size and lengths were measured using a micrometer reading to the nearest .001 inch. The dimensions shown in Table 4.5 are the averages of twenty-four different measurements for the leg sizes and eight different measurements for the weld lengths. Considerable care was exercised in making these measurements and it was felt that any errors resulting from them would be compensating errors.

The results of weld coupon tests in each group of tests appeared to be consistent except for specimens numbers 1-4 in Test Series One and 2-4 in Test Series Two. The load - deformation curves shown in Fig. 4.10 flatten out as the ultimate load is approached making it difficult to determine the exact value of the ultimate deformation. The plane of failure in each weld was inclined at approximately 45 degrees to the leg of the weld and passed through the leg of the weld. This mode of failure is consistent with previously observed modes of failure for longitudinal welds.[9,17,18]

The average weld strengths obtained from these tests were
lower than those recorded by Butler and Kulak[5]. The
coupons tested for Series One, Two, and Three had average
strengths of 9.43, 10.17 and 9.75 kips per lineal inch,
respectively. These values are based on an equivalent weld
having a 1/4 inch leg size.

5.2 Full-Size Specimen Tests

5.2.1 Load - Rotation Behaviour

The rotation gages on all specimens were intended
to measure the rotation provided by the welds. These gages
were placed as closely as possible to the test welds so that
the rotation of the beam itself would influence the readings
as little as possible. Because the rotation gages were
attached by means of spot welds it was necessary to keep them
about two inches away from the test welds so that the spot
welding would not affect the test welds. Therefore the beam
itself contributed somewhat to all the recorded rotations.

In Fig. 4.7 the load versus rotation plots are
presented for seven test specimens of Test Series One. As
can be seen, the test welds show rather large ultimate
rotations, varying from 0.015 radians to 0.025 radians. The

rotations for specimens A-2, A-6, A-7 and A-8 vary over a small range, between 0.015 and 0.017 radians, while the eccentricity to weld length ratio for these specimens varies between 1.26 and 2.02. Overall, the rotations vary from approximately 0.015 to 0.025 radians while the corresponding ratio of eccentricity to weld length varies from 1.03 to 2.03.

The load versus rotation graphs for the test specimens of Series Two and Three are shown in Figs. 4.8 and 4.9, respectively. It can be seen that the average ultimate rotation for these specimens is approximately 0.010 radians as compared to an average ultimate rotation of 0.020 radians for the specimens of Test Series One. The smaller rotation capacity in Series Two and Three is the result of the low ultimate deformations occurring in the transverse welds on the tension flanges of the specimens. It is also partly due to the larger bearing area provided by the compression flange below the neutral axis.

The corresponding load versus rotation curves of Series Two and Three compare favourably with one another, although the initial slopes of the curves for Series Two are more well-defined. This is perhaps because the additional transverse compression flange weld used in Series Three tends to make the connections more rigid in the initial stages of loading. After an "initial set" in this compression weld,

the compression flanges come into bearing with the reaction plate and, thereafter, the weld rotations become more sensitive to additional loading. In general, however, the initial slopes of the curves of Test Series Three are greater than the initial slopes of the corresponding curves of Test Series Two. For example, the initial slopes for curves C-2 and B-2 are approximately 1.67 x 10^4 kips/radian and 1.11 x 10^4 kips/radian, respectively. From this comparison it would seem that the added compression flange weld makes the specimen connections of Test Series Three initially more rigid than those of Test Series Two. However, the corresponding specimens of these two test series have approximately equal ultimate rotation capacities as well as approximately equal ultimate loads.

5.2.2 Prediction of Ultimate Loads

The theoretical prediction of the ultimate capacities of test specimens in all three test series are predominantly on the conservative side if a triangular distribution of compressive stresses in the bearing zone is used (Fig. 3.2(b)). For specimens of Test Series One using this stress distribution yields a set of random errors in predicting the ultimate loads. These errors range from

-4.7 to -16.0 per cent on the conservative side and from
+0.2 to +12.1 per cent on the unconservative side. (See
Table 5.1)

Using a triangular bearing stress distribution
for the prediction of ultimate loads for specimens of Test
Series Two and Three results in predicted ultimate loads
which are always on the conservative side. For Test Series
Two the errors range from -1.8 per cent to -16.9 per cent with
an average of -10.4 per cent. For Test Series Three the
errors range from -8.7 per cent to -17.4 per cent with an
average of -12.0 per cent.

The prediction of the ultimate loads of all
specimens tested is based on the theoretical method as outlined
in Chapter IV. Apart from the assumptions listed there,
other factors may influence the accuracy of the predicted
loads. These are:

1. For the specimens of Test Series Two and
Three, the triangular bearing stress distribution was
based on a maximum stress equal to the yield stress of the
flanges as determined from coupon tests. In the theoretical
analysis, this triangular stress block was applied to both
the flange and web of the specimen. However, it is gener-
ally true that the web of a rolled shape has a higher yield
stress value than the flange. In fact, for specimen B-2 of

Test Series Two a tensile test of a web coupon indicated a yield stress of 49.4 ksi. as opposed to a corresponding yield stress of 43.8 ksi. for the flange of the specimen. Using this higher yield stress in the analysis for specimen B-2 results in a predicted ultimate load of 31.8 kips as opposed to one of 31.4 kips using the lower yield stress of the flange. This difference represents an error of less than 2 per cent. Consequently, a full investigation in this area was not considered necessary for the remainder of the specimens.

2. In predicting the ultimate loads of the specimens, no account was taken of the frictional forces which might exist between the plates in bearing in the compression zone. It is not possible to determine to what extent these forces would become active while the continuous action of the web weld is also present. Examination does show that the inclusion of any such forces tends to make the predicted loads more conservative, as is indeed the case.

3. In the fabrication of the specimens for Test Series Two and Three, difficulty was experienced in depositing a uniform weld on the webs of the specimens, especially near the fillet junction of web to flange. As a result, the fillet weld in these areas tended to have a substantially greater leg size than the overall average leg sizes used in

the prediction of the ultimate loads. In some cases, the weld leg size on the web at the fillet was as high as 0.5 inch as opposed to an overall average leg size of about 0.3 inch. No account was made in the analysis for this larger portion of web weld in the tension zone of the test weld. Had it been considered, however, it would tend to reduce the conservative errors obtained in predicting the ultimate loads. This source of error was present to some extent also in the specimens of Test Series One. However, the location of an oversize portion of weld tended to be random in this series rather than concentrated at the ends of the weld as in Series Two and Three. The resulting error could be expected to be random also. The nature of the resulting error would depend on whether the oversize portion of weld were located in the tension zone or in the compression zone of the weld.

4. A difficulty encountered in the prediction of the ultimate loads for all specimens was the determination of a suitable bearing stress distribution to apply to the compression zone of the connections. For Test Series One, a comparison of predicted and actual test loads indicated that a triangular stress distribution was satisfactory. However, in a similar comparison for Test Series Two and Three this assumed stress distribution became questionable. As a consequence, other possibilities of bearing stress distributions were investigated and the results of this are discussed in Section 5.2.4

5. In Test Series Two and Three the additional bearing area provided by the web-to-flange fillets in the compression zone was not taken into consideration because of difficulty in accurately determining the contributory area. This area for one specimen was estimated to be only about 0.15 square inches and would seem to contribute very little to the ultimate loads. However, the effect of including this area would tend to reduce the conservative errors that were obtained in predicting the ultimate capacities of these specimens.

6. Imperfect centering and alignment of the sections on the reaction plates was noticeable in some cases. This was probably due to cooling stresses set up in the test welds as well as the fact that wide-flange sections with non-parallel flanges may have been used. In such cases the actual test specimens would not correspond exactly to the mathematical model used for the prediction of the ultimate loads. Such imperfections are virtually uncontrollable. In any event, the resulting error could be expected to be both small and random in nature.

7. As can be seen from Table 4.4 and Figure 4.10, the ultimate deformations and ultimate capacities of test welds used differed for each test series. These characteristics were determined only for control weld coupons loaded at an angle of zero degrees to the weld axis. The empirical

relationships obtained by Butler and Kulak[6] were readjusted to conform with the results of these tests. It was assumed that the ultimate capacities and ultimate deformation of elements of weld subjected to other angles of loading would vary as for those loaded at zero angle of loading. This assumption is probably not strictly correct and, if so, may produce either conservative or unconservative predictions.

8. It was estimated that the load cell and the attached micro-strain reader used to indicate actual loads applied to the specimens could be in error by as much as ±2 per cent.

5.2.3 Comparison of Ultimate Loads and Current Allowable Loads

The current allowable loads for all connections tested in the program were calculated on the basis of the principles of Method 1 as outlined in Chapter II. These loads together with the corresponding factors of safety based on the measured ultimate loads, are presented in Table 4.4. The allowable stress used in these calculations was 18.0 ksi., the current allowable value specified for welds made with E60 electrodes[10].

For the specimens tested in Series One, the factor of safety varies from 4.7 to 6.4 as the ratio of eccentricity of load to weld length varies from 2.03 to 1.03. This variation of factor of safety with ratios of eccentricity to weld length is in line with observations made by previous investigators[5].

The factors of safety obtained for the specimens of Series Two range between a minimum value of 7.5 and a maximum value of 8.4 with an average value of 8.0. For the specimens tested in Series Three the factors of safety vary between a minimum value of 5.3 and a maximum value of 5.8 with an average value of 5.6. The discrepancy between the average values of the safety factors for Series Two and Three arises from the elastic beam element concept used in the analysis of the allowable load. Although the connections of these two series of tests have approximately equal ultimate loads for corresponding wide-flange sections used, the corresponding factors of safety differ considerably. This arises because the moment of inertia of the I-shaped test weld as used in the analysis of Method 1, is about 40 per cent greater than the moment of inertia for the corresponding T-shaped weld. This leads to a lower allowable load for the T-shaped weld.

5.2.4 Ultimate Load Predictions For Different Stress Blocks

Table 5.1 summarises the predicted loads and the corresponding errors obtained for all test specimens using three different shapes of stress blocks. The use of a triangular distribution of bearing stress in the compression zone of the connection gives the best set of predicted loads throughout the three series of tests. The use of this type of stress block results in a maximum negative error of -17.4 per cent and an average value of -10.4 per cent and a maximum positive error of +12.1 per cent with an average positive error of +6.7 per cent.

The use of a parabolic bearing stress distribution gives better results for Series Two and Three. The average error in the predicted loads for specimens of Series One is increased, however. The overall average negative error using a parabolic stress block is -9.4 per cent and the average positive error is +9.3 per cent. The errors vary from a maximum negative value of -15.9 per cent to a maximum positive value of +21.2 per cent.

The best results in predicted loads for Series Two and Three are obtained when a rectangular distribution of bearing stresses is used. The errors for the predicted loads in Test Series One are greatly increased, however. The overall average negative error is -6.8 per cent and the overall average positive error is +17.6 per cent.

On the basis of this comparison, it was decided that a triangular stress distribution could be used to obtain the best results overall for the different types of weld configurations investigated.

5.2.5 Ultimate Load Tables

The ultimate loads presented in the table in Appendix C are for eccentrically loaded welded connection of a type similar to those tested in Test Series One. The table is for a 1 inch plate thickness which is assumed to have a minimum yield stress of 36 ksi. The table is valid for ¼ inch fillet welds made from E60 electrodes of minimum tensile strength. (This corresponds to an ultimate load of 10.6 kips per lineal inch for a ¼ inch weld). The ultimate weld deformation used was 0.10 inch as obtained from previous tests by Butler and Kulak[5]. In preparing the table, the computer program presented in Appendix B and based upon the analytical method presented in Chapter III was used.

TABLE 5.1(a) COMPARISON OF STRESS BLOCKS (SERIES ONE)

SPECIMEN NO.	WIDE FLANGE SECTION	ECCENTRICITY (inches)	ACTUAL TEST LOAD (kips)	TRIANGULAR STRESS BLOCK		PARABOLIC STRESS BLOCK		RECTANGULAR STRESS BLOCK	
				Predicted Load	Per Cent Error	Predicted Load	Per Cent Error	Predicted Load	Per Cent Error
A-1	10WF39	8.0	62.5	52.6	-16.0	56.6	-9.4	62.0	-0.8
A-2	10WF39	12.0	39.0	35.7	-8.5	38.6	-1.0	42.3	+8.5
A-3	10WF39	16.0	23.1	25.9	+12.1	28.0	+21.2	30.7	+32.9
A-4	10WF39	20.0	19.5	20.7	+6.1	22.3	+14.4	24.5	+25.6
A-5	10WF33	16.0	23.6	22.5	-4.7	24.5	+3.8	27.4	+16.1
A-6	10WF66	16.0	32.6	30.8	-5.5	32.8	+0.6	35.7	+9.5
A-7	12WF65	15.0	59.7	64.8	+8.5	69.5	+16.4	75.5	+26.5
A-8	12WF65	20.0	49.6	49.7	+0.2	53.5	+7.9	58.5	+17.9

TABLE 5.1(b) COMPARISON OF STRESS BLOCKS (SERIES TWO AND THREE)
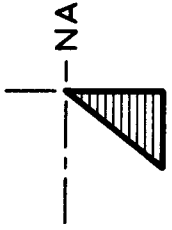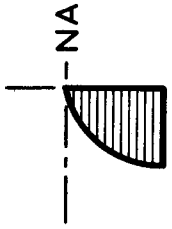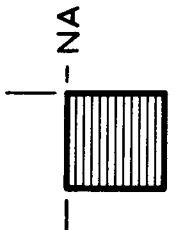
SPECIMEN NO.	WIDE FLANGE SECTION	ECCENTRICITY (inches)	ACTUAL TEST LOAD (kips)	TRIANGULAR STRESS BLOCK		PARABOLIC STRESS BLOCK		RECTANGULAR STRESS BLOCK	
				Predicted Load	Per Cent Error	Predicted Load	Per Cent Error	Predicted Load	Per Cent Error
B-1	6WF25	15.0	46.6	40.3	-13.5	41.2	-11.6	42.5	-8.7
B-2	6WF25	20.0	37.8	31.4	-16.9	32.1	-15.1	33.2	-12.2
B-3	8WF40	15.0	62.5	61.4	-1.8	62.8	+0.5	64.8	+3.7
B-4	8WF40	20.0	51.0	46.2	-9.4	47.2	-7.5	48.8	-4.4
C-1	6WF25	15.0	46.6	40.9	-12.2	41.8	-10.3	43.1	-7.5
C-2	6WF25	20.0	38.4	31.7	-17.4	32.3	-15.9	33.2	-13.5
C-3	8WF40	15.0	66.0	59.6	-9.7	61.0	-7.6	63.0	-4.5
C-4	8WF40	20.0	46.1	42.1	-8.7	43.2	-6.3	44.8	-2.8

6. S U M M A R Y   A N D   C O N C L U S I O N S

This investigation of eccentrically loaded
fillet welds was undertaken primarily;

1. To extend the method presented by Butler
and Kulak[5] for determining the ultimate strength of
eccentrically loaded fillet welds free to deform to the
case where rotational deformation is restricted in the com-
pression zone. A comprehensive testing program was used to
check the validity of the theoretical method. To investigate
the scope of application of the method, three different weld
configurations were included in the program.

2. To investigate the magnitude and variabil-
ity of the factors of safety based on the ultimate loads
obtained in the testing program. Previous investigators
(5,16,18) have observed that present design procedures
and specifications result in high and variable factors of
safety for various eccentrically loaded weld groups.

As a result of this investigation the following
conclusions have been reached:

1. An accurate, theoretical method has been
developed to predict the ultimate loads of eccentric weld
groups which are not free to rotate in the compression zone
of the connection. The method is based on an empirical

relationship for the load - deformation response of weld elements under various angles of loading. Many previous investigators[18,14] have attempted to model existing elastic theory equations for the purpose of predicting the ultimate loads of eccentric welds. The method presented herein has proved to be much more successful than any of these, however.

2. The testing program substantiates the validity of the proposed theoretical method. As a result of this program, the relative accuracy and applicability of the method have been validated. However, improvements may be forthcoming upon further investigation of a proper stress distribution to be used for the bearing stresses in the compression zone and also the interaction among the bearing stresses, the frictional stresses, and the weld stresses in that zone.

3. From a comparison of the test results and the present allowable loads it is observed that the present factors of safety for this type of connection are unjustifiably high and subject to wide variation depending on such parameters as the ratio of load eccentricity to weld length. By utilising the proposed method for predicting the ultimate loads of such connections the present factors of safety may be made more uniform and more in line with those of other structural components.
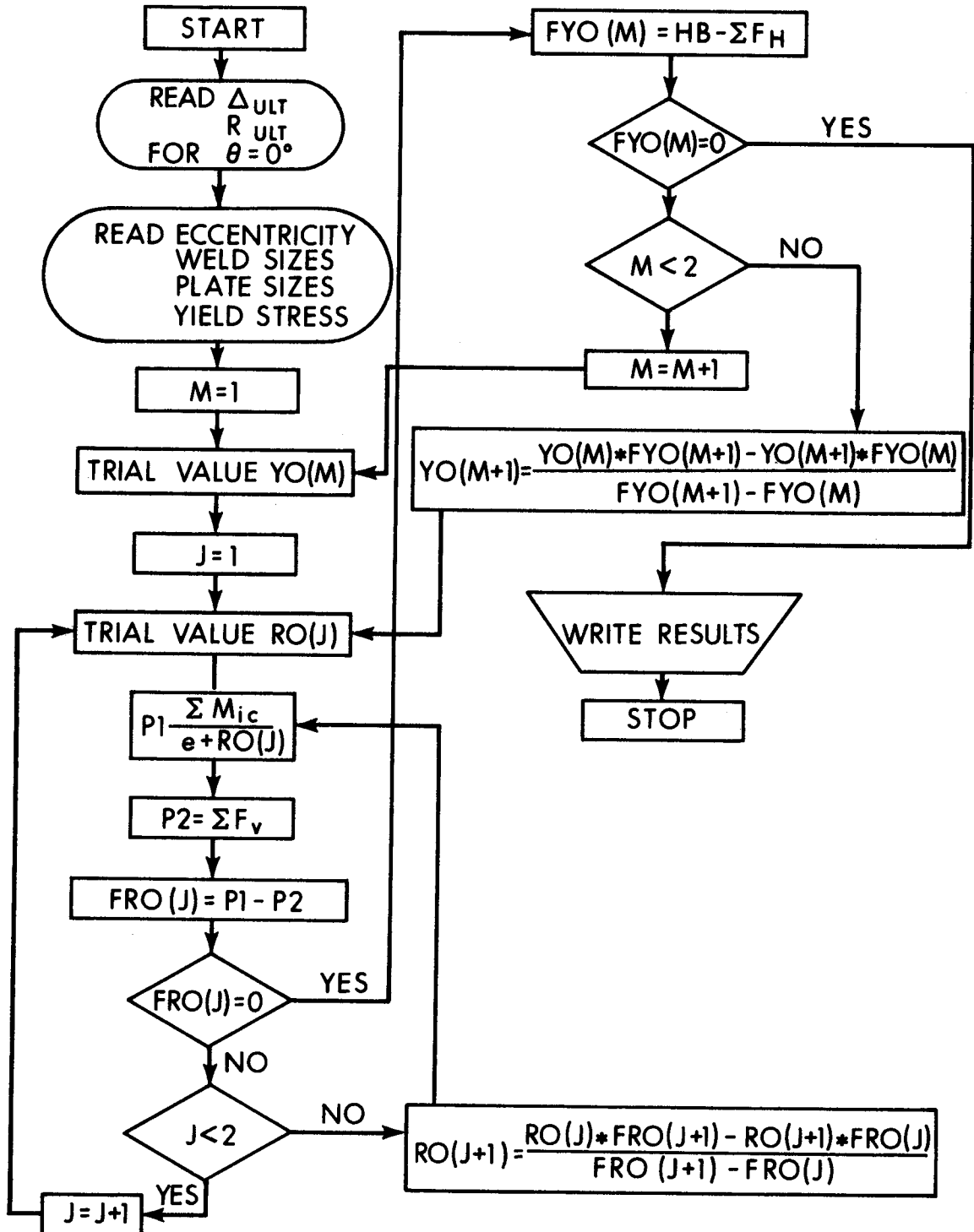
A table, presented in the Appendix, has been compiled by using the above method in a computer program. It extends the method to cover a wide range of hypothetical cases and it is hoped that this method may be used to compile an extensive design table to suit a range of practical cases.

LIST OF REFERENCES

1. American Institute of Steel Construction, Specification for the Design, Fabrication and Erection of Structural Steel for Buildings, New York, 1969.

2. ASTM "Structural Steel", American Society for Testing and Materials Standard A36-68, 1968.

3. Archer, F. E., Kitchen, E. M., and Fischer, H. K., "Strength of Fillet Welds", New South Wales University-- UNICIV, Report R6, November 1964.

4. AWS "Code for Welding in Building Construction", American Welding Society Specification No. D1.0-66, New York, 1966.

5. Butler, L. J., and Kulak, G. L., "Behavior of Eccentri- cally Loaded Welded Connections", Studies in Structural Engineering, No. 7, Nova Scotia Technical College, Halifax, N. S., September 1969.

6. Butler, L. J., and Kulak, G. L., "Strength of Fillet Welds as a Function of Direction of Load", Welding Journal Research Supplement, May 1971.

7. Brockenbrough, R. L., and Johnston, B. G., "Welded Connections", USS Steel Design Manual, Pittsburgh, Pennsylvania, November 1968.

8. CISC Handbook of Steel Construction, 2nd ed., Canadian Institute of Steel Construction, Toronto, Ontario, 1970.

9. CSA "Steel Structures for Buildings", Canadian Stand- ards Association S-16, Ottawa, Ontario, 1965.

10. CSA "Mild Steel Covered Arc-Welding Electrodes", Canadian Standards Association Standard W48.1-69, Ottawa, Ontario, 1969.

11. Conte, S. D., Elementary Numerical Analysis, McGraw-Hill Book Co., New York, 1965.

12. Crawford, S. F., and Kulak, G. L., "Eccentrically Loaded Bolted Connections", _Journal of the Structural Division_, ASCE Proceedings, vol. 97, No. ST3, March 1971.

13. Fisher, J. W., "Behaviour of Fasteners and Plates with Holes", _Journal of the Structural Division_, ASCE Proceedings, vol. 91, No. ST6, December 1965.

14. Higgins, T. R., and Preece, F. R., "Proposed Working Stresses for Fillet Welds in Building Construction", _Welding Journal_, October 1968.

15. Holtz, N. M., and Kulak, G. L., "High Strength Bolts and Welds in Load-Sharing Systems", _Studies in Structural Engineering No. 8_, Nova Scotia Technical College, Halifax, N. S., September 1970.

16. Jensen, C. D., "Combined Stresses in Fillet Welds", _Journal of the American Welding Society_, February 1934.

17. McGuire, W., _Steel Structures_, Prentice-Hall Inc., Englewood Cliffs, N. J., 1968.

18. Schreiner, N. G., "Behavior of Fillet Welds when Subjected to Bending Stresses", _Journal of the American Welding Society_, September 1935.

19. Tall, L., et al., _Structural Steel Design_, Ronald Press Co., New York, 1964.

20. Vandeperre, L. J., and Joukoff, A., _Le Calcul des Constructions Soudees_, A. de Breck, Brussels, 1939.

APPENDIX   A

START

READ Δ_{ULT}
R_{ULT}
FOR $\theta = 0°$

READ ECCENTRICITY
WELD SIZES
PLATE SIZES
YIELD STRESS

$M = 1$

TRIAL VALUE YO(M)

$J = 1$

TRIAL VALUE RO(J)

$P1 \dfrac{\Sigma M_{ic}}{e + RO(J)}$

$P2 = \Sigma F_v$

$FRO(J) = P1 - P2$

$FRO(J) = 0$ — YES

NO

$J < 2$ — NO

YES

$J = J + 1$

$RO(J+1) = \dfrac{RO(J) * FRO(J+1) - RO(J+1) * FRO(J)}{FRO(J+1) - FRO(J)}$

$FYO(M) = HB - \Sigma F_H$

$FYO(M) = 0$ — YES

NO

$M < 2$ — NO

$M = M + 1$

$YO(M+1) = \dfrac{YO(M) * FYO(M+1) - YO(M+1) * FYO(M)}{FYO(M+1) - FYO(M)}$

WRITE RESULTS

STOP

79

APPENDIX B

Computer Program for Calculating Ultimate Loads

This program is suitable for use with an IBM 360 model computer.

```
      REAL MU,LAMDA,DEL(75),RAD(75),THETA(75),RO(100),FRO(100)
      DIMENSION RV(75),RH(75),Y(75),F(75),FM(75)
      DIMENSION YO(100),FYO(100)
      READ(5,2)  DD ,PP
   2 FORMAT(2F7.4)
   7 READ(5,1) WL,ECC,SIGY,WLEG,TH2
   1 FORMAT(5F7.4)
     M=0
     IF(WL.LT.0.) STOP
     YO(1)=WL/4.
     YO(2)=3.*WL/4.
 200 CONTINUE
     J=0
     M=M+1
     UW=WL-YO(M)
     DO 21 I=1,1000
     QW=UW/FLOAT(I)
     IF(QW.LE..5) GO TO 9
  21 CONTINUE
   9 ELW=QW
     N=I
     Y(1)=ELW/2.
     RO(1)=.1
     RO(2)=50.
  25 CONTINUE
     J=J+1
     RAD(1)=SQRT(RO(J)**2+Y(1)*Y(1))
     THETA(1)=(ARSIN(Y(1)/RAD(1)))*180./3.14159
     IF(N.LT.2) GO TO 3
     DO 3 I=2,N
     Y(I)=Y(I-1)+ELW
     RAD(I)=SQRT(RO(J)**2+Y(I)**2)
     THETA(I)=(ARSIN(Y(I)/RAD(I)))*180./3.14159
```

```
    3 CONTINUE
      RTV=0.
      RTH=0.
      TRHM=0.
      DO 5 I=1,N
      DEL(I)=(DD/.105)*(RAD(I)/RAD(N))*.225*(THETA(N)+5.)**
     1(-.47)
      RULT=(10.+THETA(I))/(.92+.0603*THETA(I))
      RULT=.36799*PP*WLEG*RULT*ELW
      MU=75.*EXP(.0114*THETA(I))
      LAMDA=.4*EXP(.0146*THETA(I))
      F(I)=RULT*(1.-EXP(-MU*DEL(I)))**LAMDA
      RV(I)=(RO(J)/RAD(I))*F(I)
      RH(I)=(Y(I)/RAD(I))*F(I)
      RTV=RTV+RV(I)
      RTH=RTH+RH(I)
      TRHM=TRHM+RH(I)*Y(I)
    5 CONTINUE
      HB=SIGY*YO(M)*TH2/4.
      VB=YO(M)*RV(1)/ELW
      FRO(J)=((2./3.)*YO(M)*RTH+TRHM)/ECC-RTV-VB
      IF(J.LT.2) GO TO 25
      ERR1=(FRO(J)-FRO(J-1))/FRO(J)
      IF(ABS(ERR1).LT..01) GO TO 23
      IF(J.EQ.2) GO TO 107
      IF(FX1*FRO(J)) 108,109,109
  108 X2=RO(J)
      FX2=FRO(J)
      GO TO 110
  109 FX1=FRO(J)
      X1=RO(J)
      GO TO 110
  107 X1=RO(J-1)
      X2=RO(J)
      FX1=FRO(J-1)
      FX2=FRO(J)
  110 RO(J+1)=(X1*FX2-X2*FX1)/(FX2-FX1)
      GO TO 25
   23 FYO(M)=HB-RTH
      IF(M.LT.2) GO TO 200
      ERR2=(FYO(M)-FYO(M-1))/FYO(M)
      IF(ABS(ERR2).LT..01) GO TO 202
      IF(M.EQ.2) GO TO 117
      IF(FY1*FYO(M)) 118,119,119
  118 FY2=FYO(M)
      Y2=YO(M)
      GO TO 120
  119 FY1=FYO(M)
      Y1=YO(M)
      GO TO 120
```

```
117 Y1=YO(M-1)
    Y2=YO(M)
    FY1=FYO(M-1)
    FY2=FYO(M)
120 YO(M+1)=(Y1*FY2-Y2*FY1)/(FY2-FY1)
    GO TO 200
202 A=YO(M)
    B=RO(J)
    PULT=2.*(RTV+VB)
    WRITE(6,29)WL,ECC
 29 FORMAT('1','STEM WELD LENGTH =',F6.2,6X,'ECCENTRICITY
   1=',F6.2//)
    WRITE(6,30)SIGY,TH2
 30 FORMAT('0','YIELD POINT =',F5.2,7X,'WEB THICKNESS =',
   1F5.3//)
    WRITE(6,24) B
 24 FORMAT('0','INSTANTANEOUS CENTRE =',F8.4//)
    WRITE(6,28) A, PULT
 28 FORMAT('0','DISTANCE TO N.A. =',F8.4,4X,'ULT LOAD =',
   1F8.4/)
    GO TO 7
    END
```

APPENDIX C

ULTIMATE LOAD TABLES

L (inches)	e (inches)							
	2	4	6	8	10	12	14	16
2.00	13.26	6.64	4.47	3.35	2.66	2.22	1.95	1.70
4.00	51.88	26.37	17.61	13.23	10.54	8.82	7.56	6.62
6.00	110.70	58.90	39.47	29.68	23.73	19.79	16.86	14.86
8.00	173.80	103.51	69.92	52.57	42.11	35.11	30.16	26.34
10.00	231.93	158.05	108.54	81.99	65.69	54.81	46.98	41.10
12.00	286.75	218.57	154.93	117.57	94.38	78.76	67.57	59.17
14.00	339.36	280.78	207.71	159.16	128.16	107.12	91.93	80.48
16.00	390.20	342.28	265.36	206.30	166.77	139.59	119.90	105.03
18.00	439.84	402.11	325.67	258.14	210.06	176.15	151.49	132.73
20.00	488.59	459.80	387.36	313.69	257.57	216.72	186.57	163.69

The ultimate loads listed in this table are for hypothetical cases of eccentrically loaded welded connections of the type tested in Test Series One: L = weld length

e = eccentricity of load

P = ultimate load (kips)

83

ULTIMATE LOAD TABLES (cont'd)

L (inches)	e(inches)						
	18	20	22	24	26	28	30
2.00	1.54	1.41	1.30	1.12	1.03	0.96	0.90
4.00	5.88	5.29	4.81	4.40	4.06	3.76	3.51
6.00	13.21	11.89	10.80	9.90	9.12	8.45	7.86
8.00	23.43	21.00	19.15	17.53	16.23	15.06	14.05
10.00	36.55	32.88	29.94	27.37	25.30	23.51	21.98
12.00	52.60	47.32	43.02	39.46	36.38	33.86	31.59
14.00	71.64	64.42	58.57	53.63	49.49	45.99	42.96
16.00	93.37	84.08	76.53	70.10	64.71	60.05	56.10
18.00	118.08	106.35	96.77	88.68	81.86	76.04	70.97
20.00	145.69	131.23	119.39	109.44	101.09	93.86	87.66

The ultimate loads listed in this table are for hypothetical cases of eccentrically loaded welded connections of the type tested in Test

Series One: L = weld length

e = eccentricity of load

P = ultimate load (kips)

APPENDIX D

DEVELOPMENT OF EQUATIONS FOR A T-SHAPED WELD CONNECTION

Fig. D-1 shows a symmetrical T-shaped weld connection which, for the sake of simplicity, is considered to be composed of two identical parts as shown. In the theoretical analysis, the capacity of one of these parts is obtained. The total capacity of the connection is, of course, simply twice this amount.

Fig. D-2 shows that the length of fillet weld along the tension flange can be considered to be concentrated at one point. The total resisting force per inch of this weld is then given by equation 3.6 namely,

$$R_{ult_i} = \frac{10 + \theta_i}{0.92 + 0.0603\theta_i} \qquad 3.6$$

where θ_i = 90 degrees in this case. Since this weld is loaded at an angle of 90 degrees to its longitudinal axis, the maximum possible deformation is given by equation 3.4,

$$\Delta_{max} = 0.225(\theta_n + 5)^{-0.47} \qquad 3.4$$

where θ_n = 90 degrees.

85

The deformation of the ith element of weld is given by equation 3.5,

$$\Delta_i = \frac{r_i \Delta_{max}}{r_n} \qquad\qquad 3.5$$

where,

$$r_n = \sqrt{r_o^2 + (W_1 - y_o + t)^2} \qquad\qquad D.1$$

and where t is the flange thickness, W_1 is the length of web weld, and y_o is the distance to the neutral axis as shown in Fig. D-2.

H_b and H_{bb} are the bearing forces of the web and the flange of the specimen, respectively. Therefore,

$$H_b = \frac{\sigma_y y_o w}{4} \qquad\qquad D.2$$

and,

$$H_{bb} = \frac{\sigma_y T_1 t}{2} \qquad\qquad D.3$$

where w is the web thickness, σ_y is the yield stress of the flange, and T_1 is the flange width.

The vertical shear resistance, V_b, of the weld in the compression zone is given by,

$$V_b = \frac{y_o}{(W_1 - y_o)} \sum_1^{n-1} (R_i)_v \qquad \text{D.4}$$

in which $(R_i)_v$ is as defined in equation 3.9.

As described in Chapter III, the equations of statics must again be satisfied. In this case, it is convenient to take the sum of the moments about the flange weld. The equation is,

$$\Sigma M_{f.w.} = Pe + \sum_1^{n-1} (R_i)_h (W_1 - y_o + t - y_i) - H_b(W_1 - y_o/3 + t)$$
$$- H_{bb}(W_1 + \frac{3}{2}t) = 0 \qquad \text{D.5}$$

where $(R_i)_h$ is as defined by equation 3.10. Summing the vertical forces gives,

$$\Sigma F_v = R_n \sin\theta_t + \sum_1^{n-1} (R_i)_v + V_b - P = 0 \qquad \text{D.6}$$

where R_n is the force resisted by the flange weld and θ_t is the angle that this force makes with the horizontal.

The sum of the horizontal forces is,

$$\Sigma F_h = -R_n \cos\theta_t - \sum_1^{n-1} (R_i)_h + H_b + H_{bb} = 0 \qquad \text{D.7}$$

The solution of equations D.5, D.6, and D.7 is obtained in exactly the same manner as discussed in Chapter III for equations 3.18, 3.19, and 3.21.
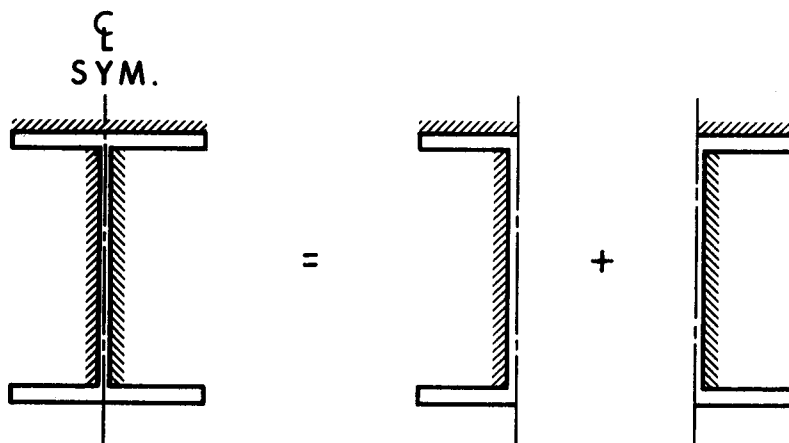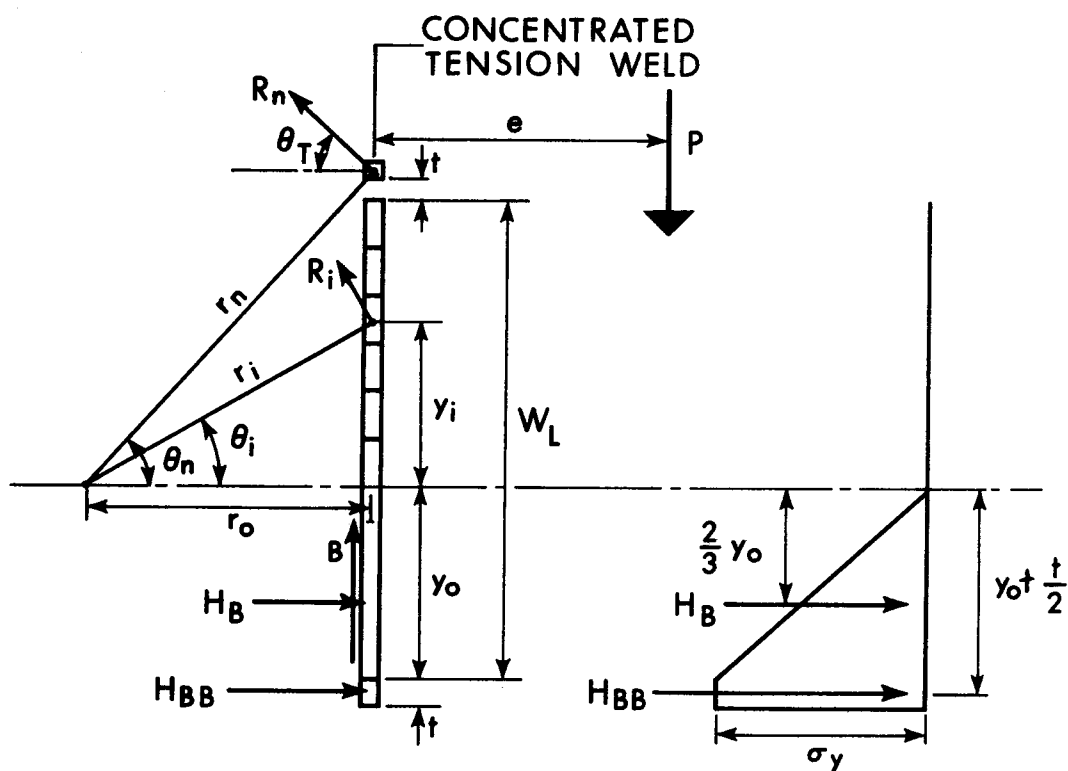
FIG. D.I SYMMETRICAL TEE-SHAPED FILLET WELD

FIG. D.2 ECCENTRICALLY LOADED TEE-SHAPED FILLET WELD